1995

Field study of currents at Norfolk Naval Shipyard, Portsmouth, Virginia

John M. Brubaker
Virginia Institute of Marine Science

Field Study of Currents at Norfolk Naval Shipyard, Portsmouth, Virginia

John M. Brubaker

School of Marine Science
Virginia Institute of Marine Science
College of William and Mary
Gloucester Point, VA 23062

Contract Report to
SCS Engineers
Reston, VA

Contract No. N62470-92-D-6450

April 1995

INTRODUCTION

As a component of an investigation into biofouling problems near the Norfolk Naval Shipyard, a field study of currents was conducted in the Southern Branch of the Elizabeth River in the vicinity of the shipyard's aircraft carrier slips. The objective of this study was to determine the magnitude and direction of currents in an area encompassing the turning basin adjacent to the slips, and the transitional regions to the north and south where the river tapers from a width of approximately 600 m in the turning basin to its more typical width of 150 m. To the north, the transition is gradual; to the south it is abrupt.

Design of a sampling strategy capable of providing a useful characterization of the currents requires consideration of the expected scales of variability in spatial dimensions and in time. Bottom friction and density stratification may cause vertical current shear, and the geometry of the region would be expected to impose lateral (cross-river) and longitudinal (along-river) variations in the flow, so three-dimensional sampling in space is required. Various time scales of variability are likely to be present in the flow field, but tidal oscillations are fundamental and energetic, and failure to account for them can confound attempts to understand the effects of non-tidal forcing (by the wind, for example). Key tidal time scales are the ~ 12 h period of semi-diurnal current oscillations, and the fortnightly spring-neap modulation of the oscillation amplitude.

Sampling at intervals of order 1 m in the vertical, 100 m in both horizontal dimensions, and 1 h in time would be highly effective in resolving the structure of the flow field over a semi-dirunal cycle. In principle, an array of several hundred moored current meters could provide the desired sampling, but even if the cost of such a deployment were not prohibitive, heavy shipping traffic in the region would preclude it.

Acoustic Doppler current measurement technology, with its capability for underway measurement, can acquire a set of vertical profiles of water velocity, spaced at selected horizontal intervals along the sampling path. By traversing a circuit or grid of survey lines, three dimensional variability can be sampled, and by executing repeated surveys, temporal evolution of the flow can be resolved.

The following sections describe field deployments of an acoustic Doppler current profiler (ADCP), analysis of the resulting data to produce vector flow maps for each of 21 separate surveys of the region, further processing and tidal harmonic analysis to extract the non-tidal residual flow field, and a discussion of the results.

FIELD PROGRAM

Timing of the field studies was based on the need to sample semi-diurnal and spring-neap variability. Clear amplitude modulation occurs over some spring-neap periods, while it is hardly noticeable over others. A strong contrast was indicated in tidal predictions for early February 1995, and sampling was scheduled for 1 February (spring tide) and 8 February (neap tide). As shown in Figure 1, predicted maximum currents at Chesapeake, just south of the turning basin, were greater on the 1st than the 8th by a factor of two (ebb) to five (flood).

Currents were measured with a 1200 kHz acoustic Doppler current profiler (model DR, RD Instruments), towed in a catamaran vehicle by the R/V Langley. The tow line and fixed rudders on the catamaran were configured so that the adcp followed alongside the vessel, well away from wake influence. Raw current velocity data, recorded in the field at 1.2 s intervals, consisted of 4-ping averages of along-beam velocity components.

Satellite navigation data, provided by a differential GPS system and tagged with the sequential number of the most recently acquired ADCP ping ensemble, were recorded at 6 s intervals.

Several repeated surveys over a 12 h period would be required in order to resolve the semi-diurnal cycle. It was determined that, at a towing speed of 4-5 knots (2-2.5 m/s), a sampling circuit that would provide adequate spatial coverage could be traversed in a time interval of order 1 h. Allowing for turnaround between surveys, approximately 10 separate surveys could be executed on each sampling day. As anticipated, following a predetermined sampling circuit was impossible, due to vessel traffic in the area. Instead, the path was adjusted in real time according to the exigencies of each survey. Several examples, the first four surveys of each sampling day, are shown in Figure 2. Ten complete surveys were completed on 1 February and 11 on 8 February.

Low resolution bathymetric data were collected in the study area. With respect to topographic variability that might significantly influence the flow field, the bottom was relatively flat and featureless.

DATA ANALYSIS

Primary Processing

With the ADCP system used in this study, a single acoustic ping produces a vertical profile of current velocity data throughout the usable portion of the water column in a fraction of a second. However, the error associated with single-ping data is unacceptably large, approximately 13 cm/s. Averaging over time reduces the error by the inverse square root of the number of pings averaged, but a tradeoff against horizontal resolution arises, as longer averaging intervals correspond to longer segments of sampling track. A good compromise was reached with 30-s averages. Typically, these contained 100 pings, reducing the error to approximately 1.3 cm/s, and at vessel speeds of 2 to 2.5 m/s, the corresponding segment of track over which data were averaged was 60 to 75 m.

For each 30-s sample, velocity components were rotated from the measurement coordinate system, in which directions are referred to magnetic north, into east and north components referred to true north. ADCP "bottom-track" velocity data were subtracted from raw water column velocities to remove the apparent current contribution of underway sampling. High quality bottom track data were obtained throughout the field study.

Position fixes for each velocity profile were determined by taking the midpoint time of the 30-s average, and finding the corresponding latitude and longitude within the 6-s GPS navigation files by linear interpolation. Each circle on the survey tracks shown in Figure 2 represents the midpoint of a segment of trackline corresponding to a 30-s average current profile.

Tidal Harmonic Analysis

In order to enhance and clarify the interpretation of the flow fields determined on the individual current surveys, further analysis was undertaken. Although tidal harmonic analysis is more commonly applied to time series of velocity data sampled at equal time intervals by stationary, moored current

meters, a least-squares approach to the analysis can treat irregularly spaced time series as well. By combining the data from the multiple surveys conducted over a tidal cycle, such time series can be formed from selected samples of the underway-acquired ADCP data.

The study area was partitioned into a grid of rectangular cells, each 0.001 degree of longitude by 0.001 degree of latitude. For each cell, all surveys for a sampling day were scanned for samples at locations that fell within the cell. Cells in which too few samples had been collected over the day were dropped; ultimately a grid of 35 cells, shown in Figure 3, was chosen. Typically, each survey contributed several samples to each cell. With 10 surveys on 1 February and 11 on 8 February, a suitable length time series for analysis was thus formed for each cell for each day.

For harmonic analysis, the current at a given location (a particular depth at a particular cell) was assumed to be of the form:

$$(u, v) = (U_o, V_o) + \sum_{i=1}^{n} \left(U_i \cos(\omega_i t - \phi_{Ui}), V_i \cos(\omega_i t - \phi_{Vi}) \right)$$

i.e., the sum of a non-tidal residual flow (U_o, V_o) and a set of n harmonic components representing tidal constituents with frequencies ω_i, amplitudes U_i and V_i, and phases ϕ_{Ui} and ϕ_{Vi}. u and v terms apply to the eastward and northward components respectively.

Two separate least-squares analyses were performed at each of 9 depth levels at each of the 35 cells for each of the 2 sampling days. The first analysis included only the M2 semi-diurnal tidal constituent, and the second included the M2 as well as the overtide M4. The M2 constituent was clearly dominant, and the residual flow field was substantially the same in the two analyses.

RESULTS

Individual surveys of the flow field (vector maps in Appendix)

Ten separate current surveys in the study area were conducted at spring tide on 1 February 1995, and 11 surveys were conducted a week later at neap tide on 8 February 1995. Vector maps portraying the flow field observed on each survey have been produced by plotting a current vector

emanating from the location of each (30-s average) data point along the sampling trackline. Note that these are not truly synoptic maps; the flow field may have evolved somewhat during the time required to execute a survey. However, all surveys except for the first two on 1 February were completed in less than one hour, a relatively small time interval compared to the 12.4 h period of the dominant M2 tidal constituent.

The survey vector maps are presented in pairs, one above the other, representing the flow pattern observed at two different depths during the same survey. The ADCP data were acquired as weighted averages over 2 m vertical intervals, or bins. Bins 2 and 8 were centered at depths of 3 and 9 m respectively. The date and time span (EST) of the survey is indicated at the top of each plot; for convenience, surveys will be referred to in the following discussion by the starting time.

Spring tide

Sampling on 1 February (spring tide) began at the time of predicted maximum flood current. During survey 0721, the upper level (bin 2) flow was in flood over virtually the entire study domain. The deeper flow (bin 8) was flooding at a somewhat reduced speed and, near the southern end of the region, turned more apparently toward the southward continuation of the river at the southeast corner than did the upper flow. The flood flow was weaker during the 0906 survey and had turned to ebb over much of the area by the time of the 1038 survey. In the 1142 survey, the developing jet of maximum ebb flow followed a gentle "S" curve through the region.

As the tidal current approached maximum ebb, flow in much of the turning basin became dominated by a large, persistent, counter-clockwise rotating eddy, remarkably well defined in the next four surveys spanning the time interval 1238 - 1702 h EST. In the 1613 survey, with ebb flow waning, the strongest currents in the upper flow were associated with the eddy.

During the final two surveys (beginning at 1727 and at 1846 h) of the spring tide sampling series, the flood phase became established. There appear to be vestiges of the eddy in the 1727 survey results, but these had dissipated by 1846. Predicted maximum flood, corresponding to the tidal phase at which the first survey of the day was conducted, was at 1957 h. Note that the combination of

coherent flow through the region during flood, with the recirculating eddy flow during ebb, results in flow near the entrances to the carrier slips that is generally southward over most of the tidal cycle.

Neap tide

Sampling at neap tide, 8 February 1995, began near the time of predicted maximum ebb. During the 0739 survey, a weak but identifiable jet flowed through the area in an S-curve pattern both at the upper and deeper levels. In the upper level flow, counter rotating eddies appeared on the two sides of the jet, with the southern eddy similar to the one observed during ebb at spring tide. In the deeper flow, only the southern eddy was observed. Somewhat weaker and less well defined, this pattern persisted into the 0855 survey during waning ebb.

In surveys beginning at 0959, 1105, 1210, and 1315 h, some generally flood-directed flow was observed, somewhat confined to sub-areas of the region, in contrast to the stronger, more coherent flood flow throughout the region during spring tide. Note the concentration of flood current against the eastern shore during the 1315 survey, and the appearance of a *clockwise* southern eddy in the 1450 survey, especially in the deeper flow. In the latter survey results, the deeper flow has substantially turned to ebb while the upper flow was weaker and less organized.

Over the remaining surveys, the deeper flow ebbed through the region, generally exhibiting the previously noted S-curve pattern that seems to be a characteristic feature of the ebb phase. During this same period, the upper flow generally did not develop into a well-defined ebb, perhaps responding to surface wind stress, which had a southward component most of the day.

Non-tidal residual flow

The sequences of flow maps derived from individual current surveys provide a direct representation of the evolution of the complex flow in the study area through a semi-diurnal tidal cycle, and have served to illustrate the significant differences between the stronger and weaker currents of spring and neap tide. It can be informative as well to attempt to extract from the total observed flow the less energetic non-oscillating component, i.e., the non-tidal residual, often masked by the dominant

periodic tidal currents. This may be especially relevant to considerations of long-term transport over many tidal cycles.

Vector maps depicting the residual flow field at several depth levels have been produced for each sampling day (Figure 4a-b). The mid-depth of each ADCP bin, in meters, is equal to the bin number + 1. Thus, the four levels shown correspond to depths of 3, 5, 7, and 9 m. Note that the vector lengths have been magnified relative to the scale used in the individual survey vector maps in order to accommodate the weaker residual flow magnitudes.

A prominent feature of the residual flow derived for 1 February (spring tide) is the counter-clockwise eddy flow in the southern half of the basin. The eddy is remarkably coherent and well defined, and evident at all depth levels, although the center of rotation appears further west with increasing depth. In the northern end of the region, all of the upper level flow is southward, but the deeper flow (bin 8) is northward on the west side, and southward on the east side.

The residual flow field derived from the 8 February (neap tide) current data differs significantly from the spring tide pattern, most notably in the absence of an identifiable rotational eddy corresponding to the one described above. A clockwise rotation is apparent at approximately 36.816 °N, 76.292 °W, but only in the upper, bin 2 flow map. At the deeper levels, the S-curve flow noted in the individual surveys during ebb flow, emerges as a salient feature of the neap tide residual flow. Near the carrier slips, the residual flow is essentially slack, in contrast to spring conditions.

SUMMARY

The vector maps resulting from the 21 individual current surveys constitute a relatively high-resolution determination of the fully three-dimensional, time-dependent flow field in the study area. A distinct ebb-flood asymmetry in the tidal flow was found, with a large, well defined eddy developing during ebb when strong currents entered the turning basin area from the south. Apparently, the width variation to the north of the turning basin was gradual enough to prevent such flow separation during flood. There was evidence of the ebb eddy in surveys at neap tide, but it was stronger and more clearly

defined in the spring tide results. The neap tide surveys showed that with weak tidal current amplitude, a well developed flood flow through the region may not form at all in some cycles; the neap data may also provide information on the extent to which surface wind stress can delay or inhibit tidal currents in the upper layers, with a consequent modification to the deep flow.

The sampling strategy employed in this study provided a data set with adequate spatial and temporal coverage to permit a tidal harmonic analysis to be performed at more than 300 locations in a three-dimensional array of cells filling most of the volume of the study region. From this analysis, the 3-D structure of the mean, or non-tidal residual, flow was resolved, showing with high definition a large eddy dominating the spring tide residual flow. That the eddy does not appear in the neap residual flow pattern may imply that the current regimes of the two sampling days bracketed the condition for its stable development.

This field study has documented a flow that is complex, yet characterized by some well defined features. Further study of the present data set is recommended. Additional analysis would help elucidate the potential role of the observed flow characteristics in controlling transport to and from the study area, and would provide a basis for determining whether further field study is warranted, and if so, what measurements would be most effective.

FIGURE CAPTIONS

Figure 1. Predicted tidal currents at the southern end of the study region, latitude 36.81 °N.

Figure 2. Representative survey ship tracks. (a) First four surveys on 1 February 1995 (spring tide). (b) First four surveys on 8 February 1995 (neap tide).

Figure 3. The grid of cells used in the least-squares tidal harmonic analysis. Numbered dots indicate the center of each rectangular cell (0.001 degree of longitude by 0.001 degree of latitude).

Figure 4. Vector maps of the residual flow field at four depths (depth in meters is equal to the indicated bin number + 1). The harmonic analysis included only the residual and the M2 semi-diurnal tidal constituent. (a) 1 February 1995 (spring tide). (b) 8 February 1995 (neap tide).

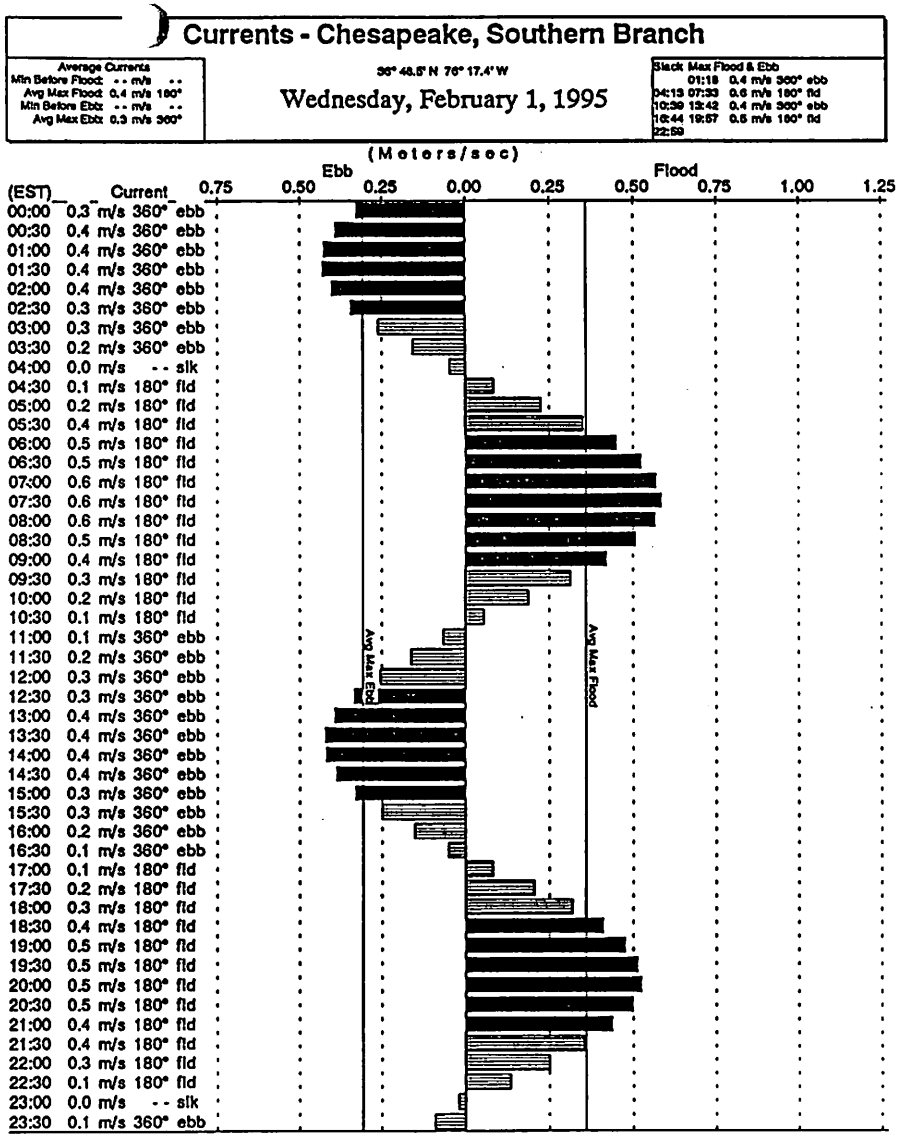
Currents - Chesapeake, Southern Branch
Average Currents
Min Before Flood: -- m/s --
Avg Max Flood: 0.4 m/s 180°
Min Before Ebb: -- m/s --
Avg Max Ebb: 0.3 m/s 360°
36° 46.5' N 76° 17.4' W
Wednesday, February 1, 1995
Slack Max Flood & Ebb
01:18 0.4 m/s 360° ebb
04:13 07:33 0.6 m/s 180° fld
10:39 13:42 0.4 m/s 360° ebb
16:44 19:57 0.5 m/s 180° fld
22:59
(Meters/sec)
Ebb
Flood
0.75 0.50 0.25 0.00 0.25 0.50 0.75 1.00 1.25
(EST) Current
00:00 0.3 m/s 360° ebb
00:30 0.4 m/s 360° ebb
01:00 0.4 m/s 360° ebb
01:30 0.4 m/s 360° ebb
02:00 0.4 m/s 360° ebb
02:30 0.3 m/s 360° ebb
03:00 0.3 m/s 360° ebb
03:30 0.2 m/s 360° ebb
04:00 0.0 m/s -- slk
04:30 0.1 m/s 180° fld
05:00 0.2 m/s 180° fld
05:30 0.4 m/s 180° fld
06:00 0.5 m/s 180° fld
06:30 0.5 m/s 180° fld
07:00 0.6 m/s 180° fld
07:30 0.6 m/s 180° fld
08:00 0.6 m/s 180° fld
08:30 0.5 m/s 180° fld
09:00 0.4 m/s 180° fld
09:30 0.3 m/s 180° fld
10:00 0.2 m/s 180° fld
10:30 0.1 m/s 180° fld
11:00 0.1 m/s 360° ebb
11:30 0.2 m/s 360° ebb
12:00 0.3 m/s 360° ebb
12:30 0.3 m/s 360° ebb
13:00 0.4 m/s 360° ebb
13:30 0.4 m/s 360° ebb
14:00 0.4 m/s 360° ebb
14:30 0.4 m/s 360° ebb
15:00 0.3 m/s 360° ebb
15:30 0.3 m/s 360° ebb
16:00 0.2 m/s 360° ebb
16:30 0.1 m/s 360° ebb
17:00 0.1 m/s 180° fld
17:30 0.2 m/s 180° fld
18:00 0.3 m/s 180° fld
18:30 0.4 m/s 180° fld
19:00 0.5 m/s 180° fld
19:30 0.5 m/s 180° fld
20:00 0.5 m/s 180° fld
20:30 0.5 m/s 180° fld
21:00 0.4 m/s 180° fld
21:30 0.4 m/s 180° fld
22:00 0.3 m/s 180° fld
22:30 0.1 m/s 180° fld
23:00 0.0 m/s -- slk
23:30 0.1 m/s 360° ebb
Avg Max Ebb
Avg Max Flood
Nautical Software (503) 579-1414

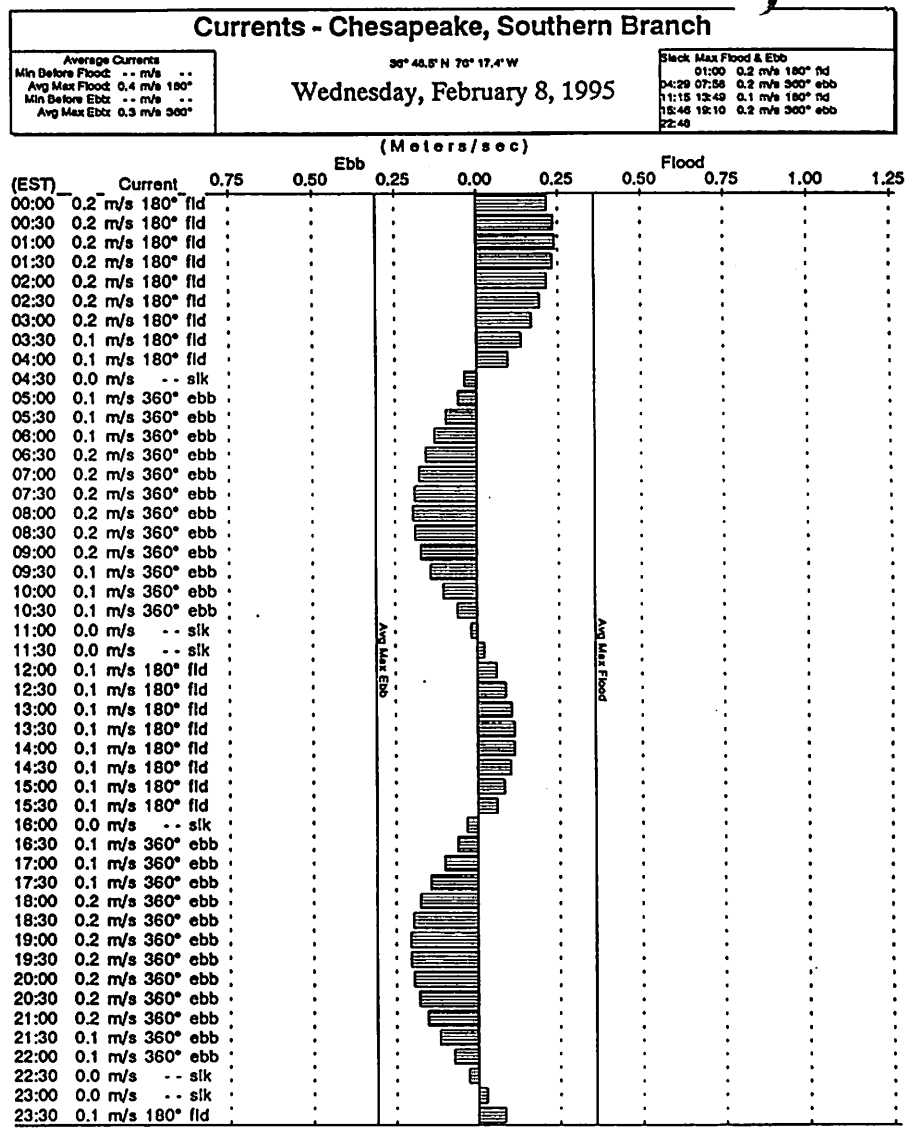
Currents - Chesapeake, Southern Branch
Average Currents
Min Before Flood: -- m/s --
Avg Max Flood: 0.4 m/s 180°
Min Before Ebb: -- m/s --
Avg Max Ebb: 0.3 m/s 360°
36° 46.5' N 76° 17.4' W
Wednesday, February 8, 1995
Slack Max Flood & Ebb
01:00 0.2 m/s 180° fld
04:29 07:56 0.2 m/s 360° ebb
11:15 13:49 0.1 m/s 180° fld
18:46 19:10 0.2 m/s 360° ebb
22:48
(Meters/sec)
Ebb
Flood
0.75 0.50 0.25 0.00 0.25 0.50 0.75 1.00 1.25
(EST) Current
00:00 0.2 m/s 180° fld
00:30 0.2 m/s 180° fld
01:00 0.2 m/s 180° fld
01:30 0.2 m/s 180° fld
02:00 0.2 m/s 180° fld
02:30 0.2 m/s 180° fld
03:00 0.2 m/s 180° fld
03:30 0.1 m/s 180° fld
04:00 0.1 m/s 180° fld
04:30 0.0 m/s -- slk
05:00 0.1 m/s 360° ebb
05:30 0.1 m/s 360° ebb
06:00 0.1 m/s 360° ebb
06:30 0.2 m/s 360° ebb
07:00 0.2 m/s 360° ebb
07:30 0.2 m/s 360° ebb
08:00 0.2 m/s 360° ebb
08:30 0.2 m/s 360° ebb
09:00 0.2 m/s 360° ebb
09:30 0.1 m/s 360° ebb
10:00 0.1 m/s 360° ebb
10:30 0.1 m/s 360° ebb
11:00 0.0 m/s -- slk
11:30 0.0 m/s -- slk
12:00 0.1 m/s 180° fld
12:30 0.1 m/s 180° fld
13:00 0.1 m/s 180° fld
13:30 0.1 m/s 180° fld
14:00 0.1 m/s 180° fld
14:30 0.1 m/s 180° fld
15:00 0.1 m/s 180° fld
15:30 0.1 m/s 180° fld
16:00 0.0 m/s -- slk
16:30 0.1 m/s 360° ebb
17:00 0.1 m/s 360° ebb
17:30 0.1 m/s 360° ebb
18:00 0.2 m/s 360° ebb
18:30 0.2 m/s 360° ebb
19:00 0.2 m/s 360° ebb
19:30 0.2 m/s 360° ebb
20:00 0.2 m/s 360° ebb
20:30 0.2 m/s 360° ebb
21:00 0.2 m/s 360° ebb
21:30 0.1 m/s 360° ebb
22:00 0.1 m/s 360° ebb
22:30 0.0 m/s -- slk
23:00 0.0 m/s -- slk
23:30 0.1 m/s 180° fld
Avg Max Ebb
Avg Max Flood
Nautical Software (503) 579-1414

Figure 1

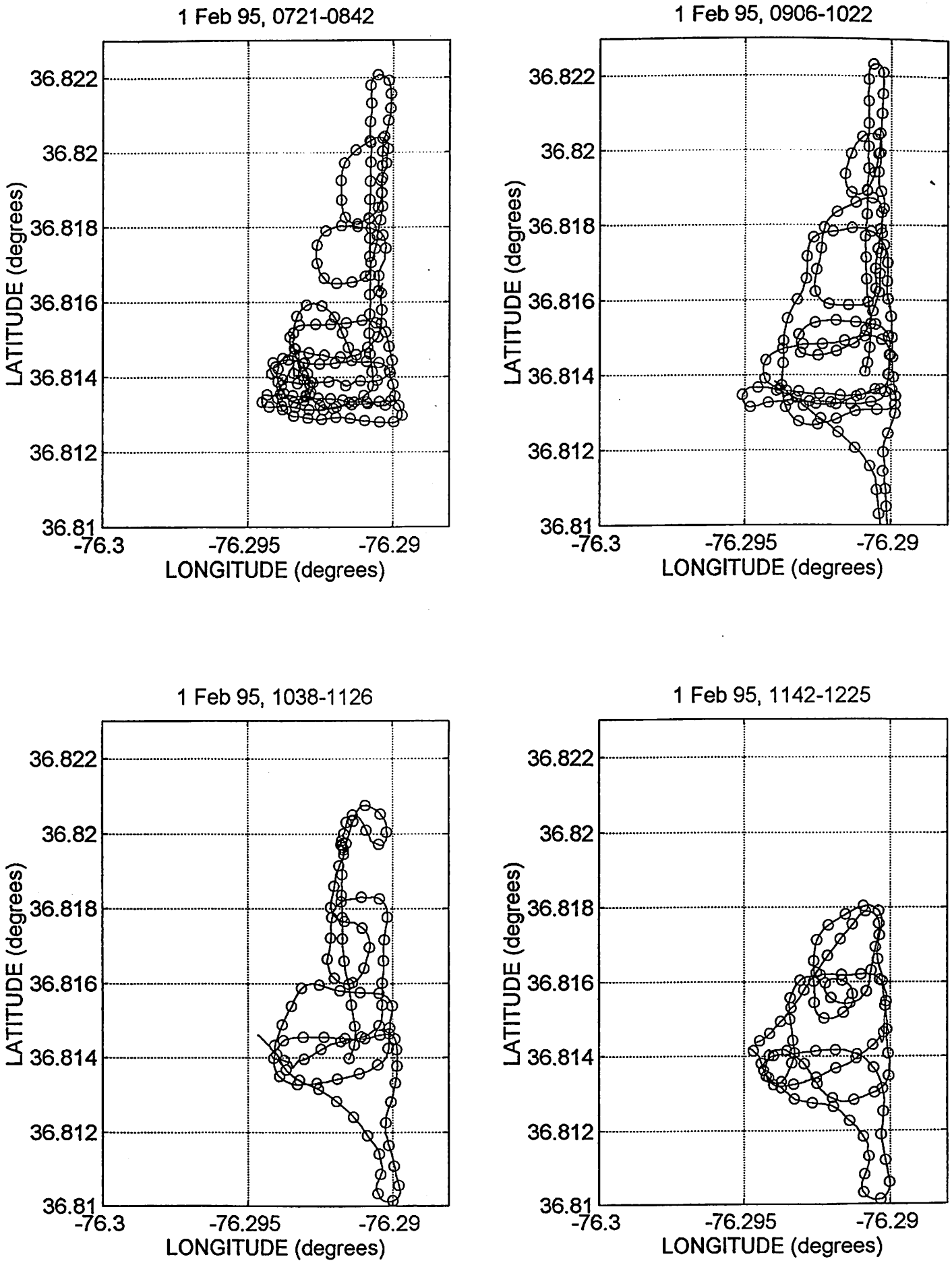
1 Feb 95, 0721-0842
1 Feb 95, 0906-1022
1 Feb 95, 1038-1126
1 Feb 95, 1142-1225
LATITUDE (degrees)
LONGITUDE (degrees)
36.822
36.82
36.818
36.816
36.814
36.812
36.81
-76.3
-76.295
-76.29

Figure 2(a)

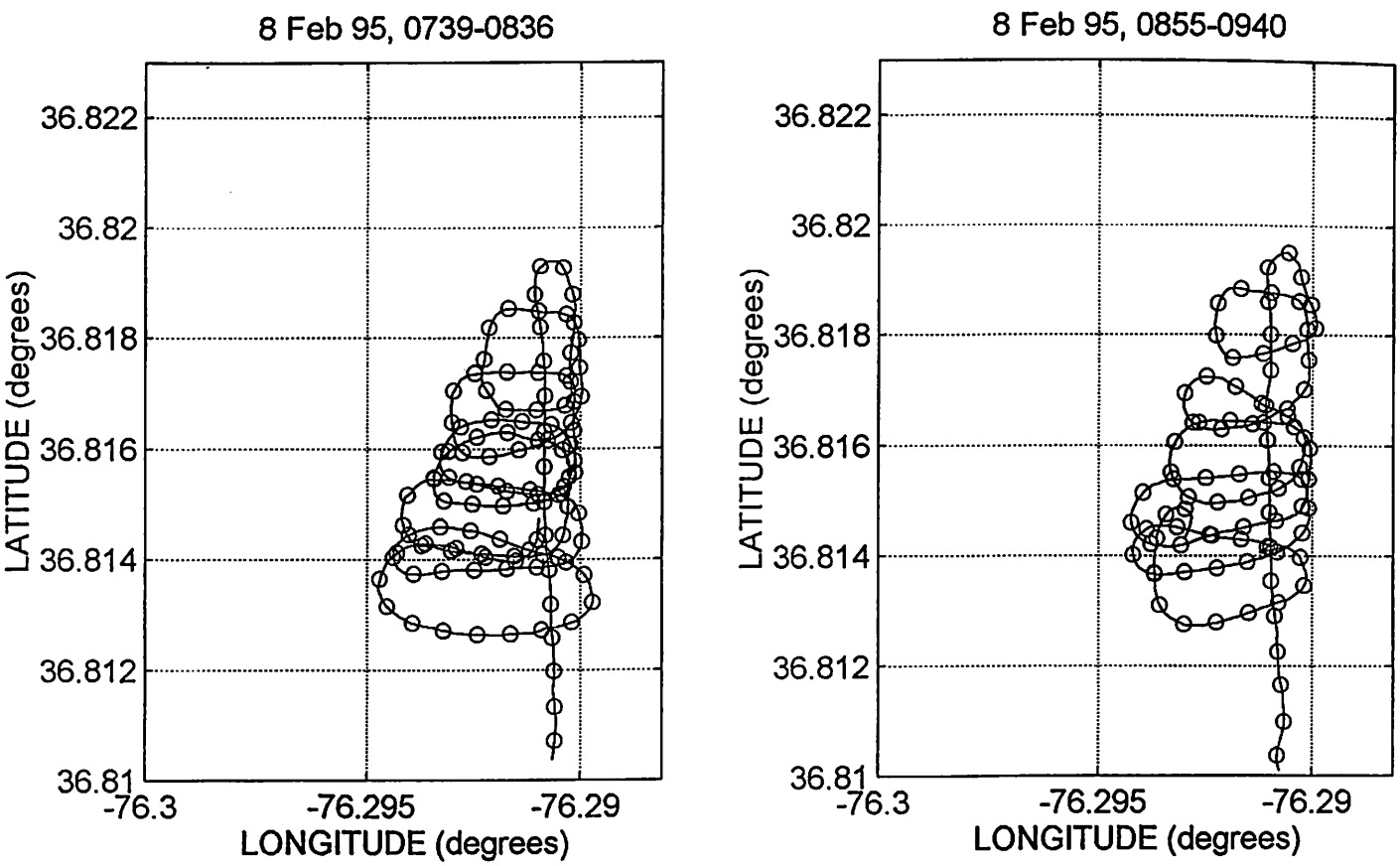
8 Feb 95, 0739-0836
8 Feb 95, 0855-0940
36.822
36.82
36.818
36.816
36.814
36.812
36.81
LATITUDE (degrees)
-76.3
-76.295
-76.29
LONGITUDE (degrees)

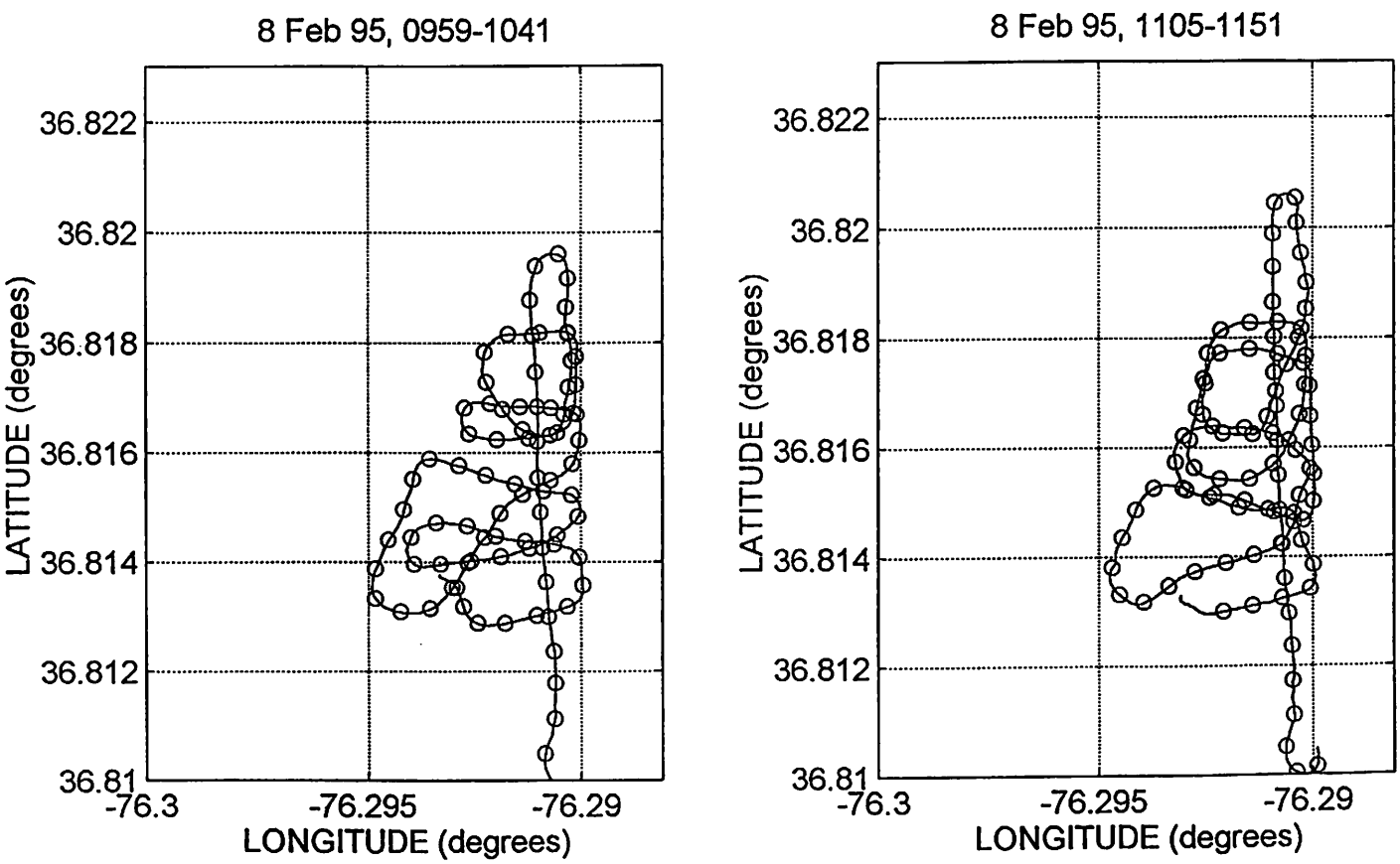
8 Feb 95, 0959-1041
8 Feb 95, 1105-1151
36.822
36.82
36.818
36.816
36.814
36.812
36.81
LATITUDE (degrees)
-76.3
-76.295
-76.29
LONGITUDE (degrees)

Figure 2(b)

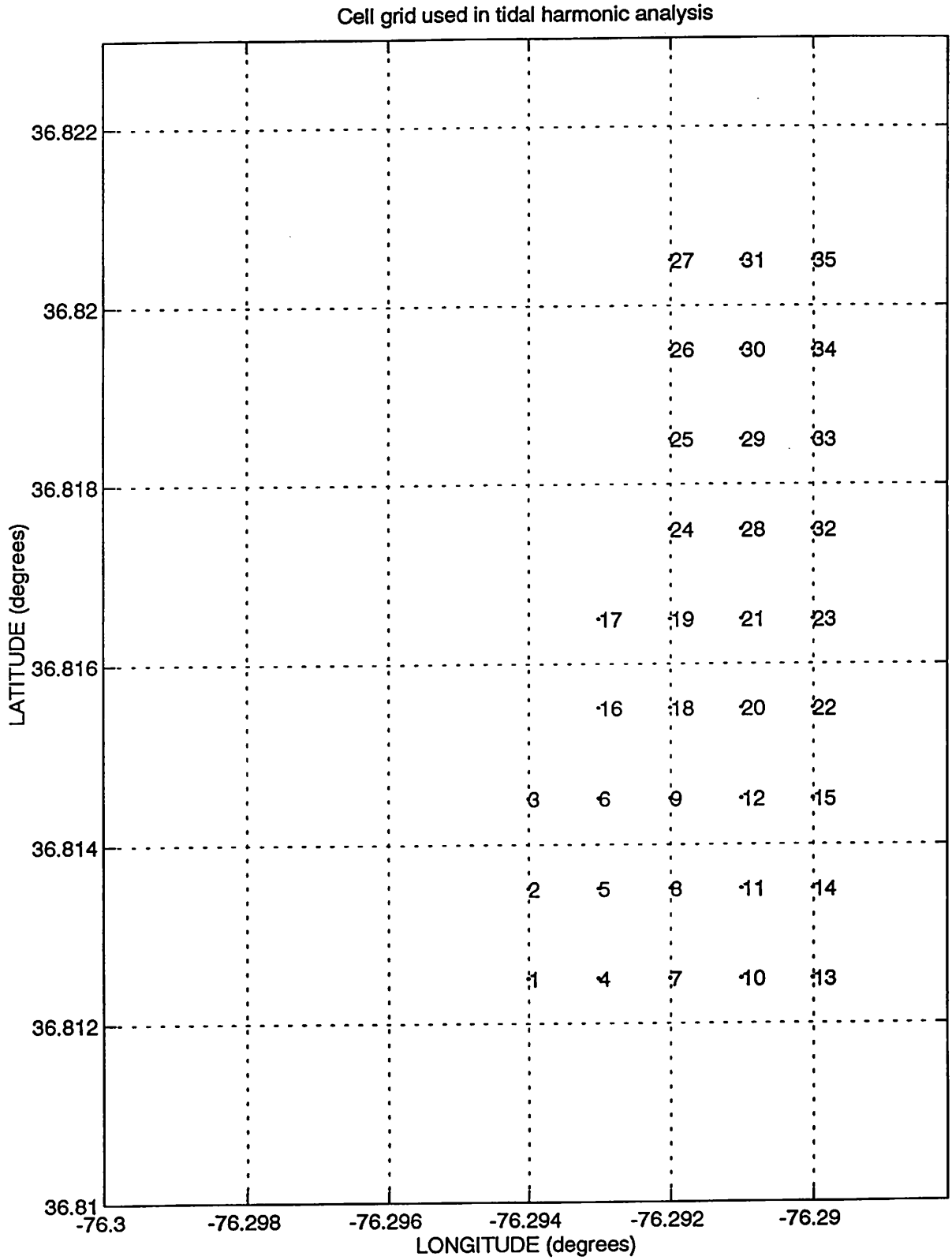
Cell grid used in tidal harmonic analysis
36.822
36.82
36.818
36.816
36.814
36.812
36.81
LATITUDE (degrees)
-76.3
-76.298
-76.296
-76.294
-76.292
-76.29
LONGITUDE (degrees)
27
31
35
26
30
34
25
29
33
24
28
32
17
19
21
23
16
18
20
22
3
6
9
12
15
2
5
8
11
14
1
4
7
10
13

Figure 3

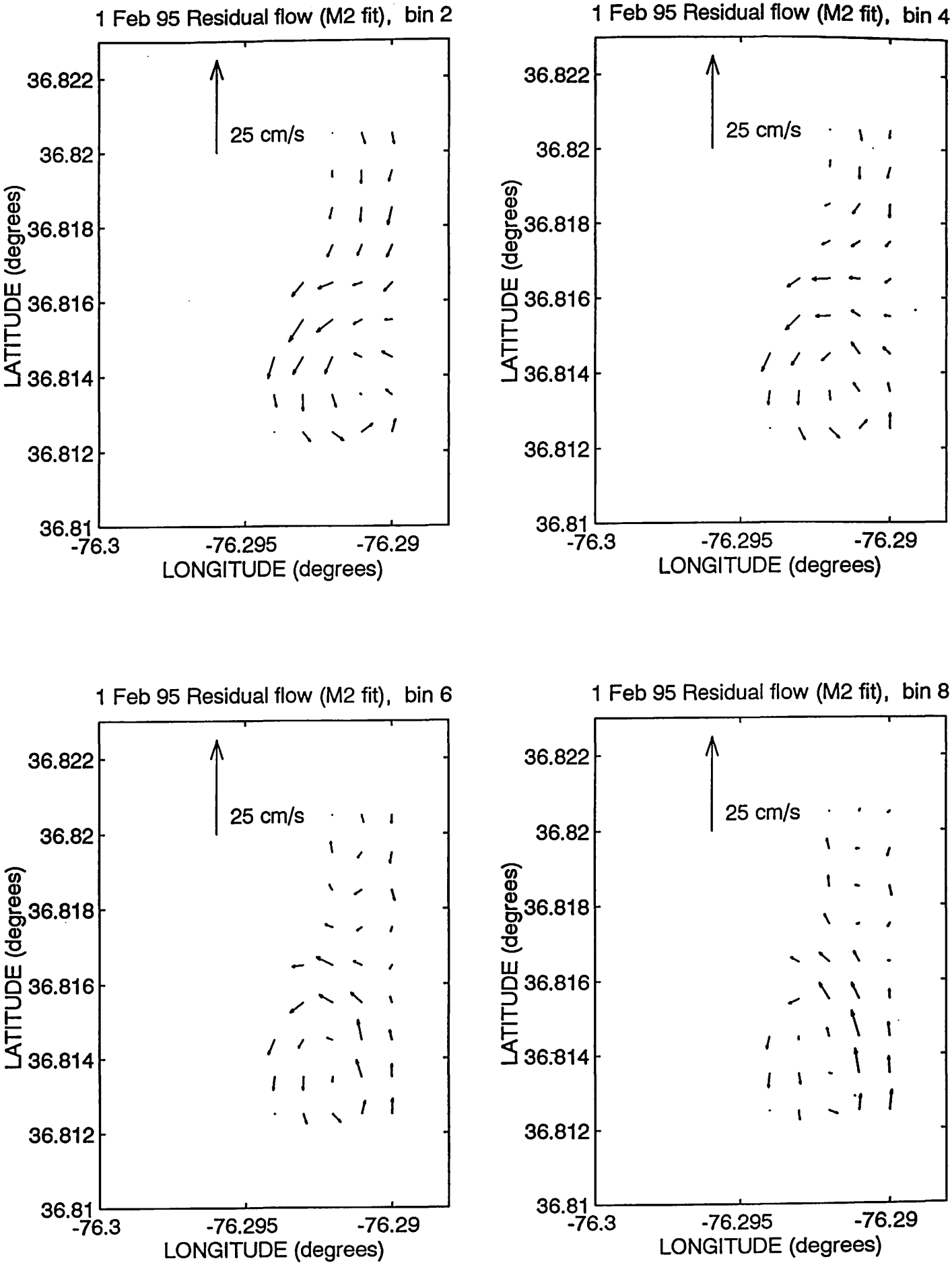
1 Feb 95 Residual flow (M2 fit), bin 2
1 Feb 95 Residual flow (M2 fit), bin 4
1 Feb 95 Residual flow (M2 fit), bin 6
1 Feb 95 Residual flow (M2 fit), bin 8
25 cm/s
LATITUDE (degrees)
LONGITUDE (degrees)
36.822
36.82
36.818
36.816
36.814
36.812
36.81
-76.3
-76.295
-76.29

Figure 4(a)

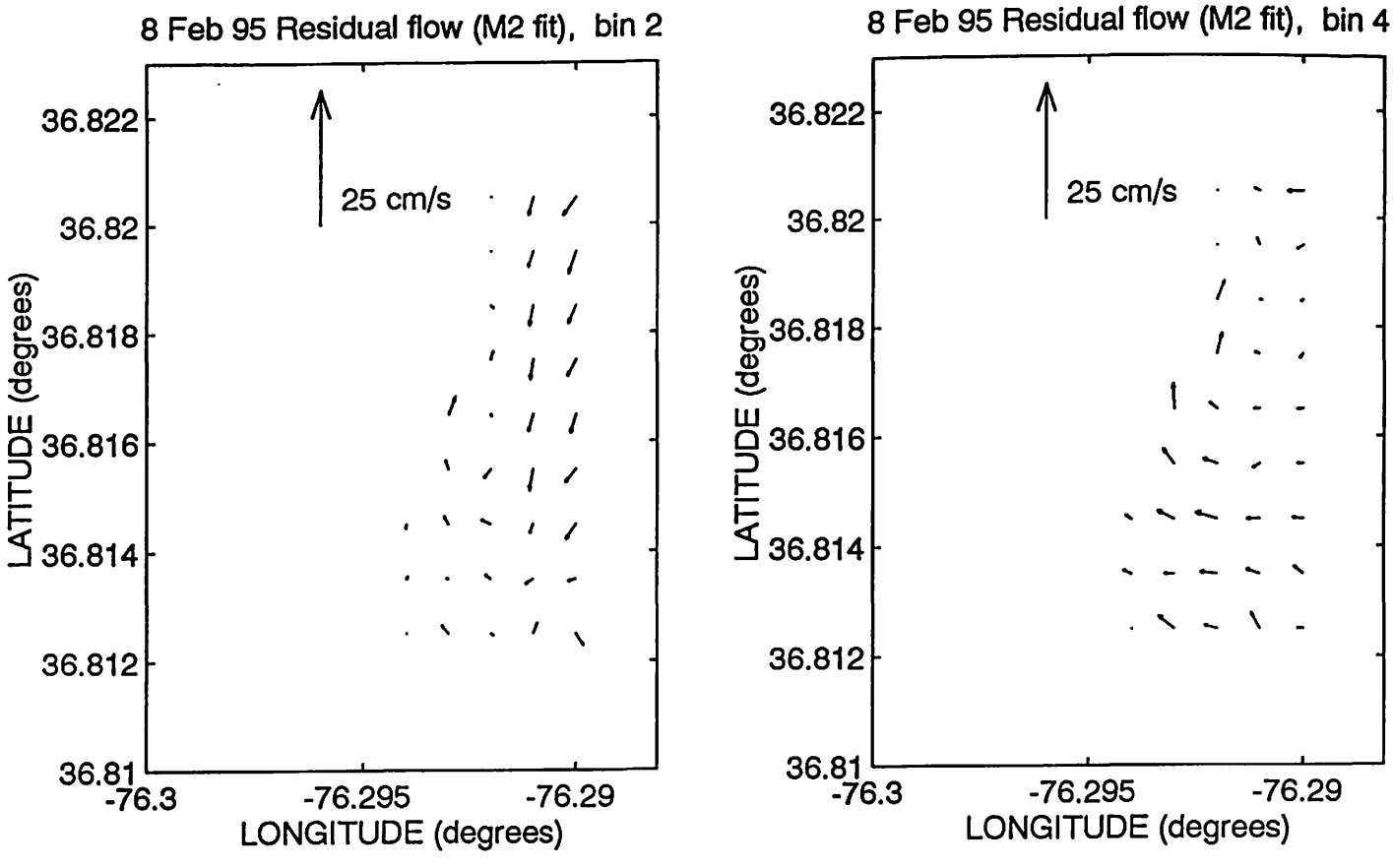
8 Feb 95 Residual flow (M2 fit), bin 2
8 Feb 95 Residual flow (M2 fit), bin 4
25 cm/s
LATITUDE (degrees)
LONGITUDE (degrees)
36.822
36.82
36.818
36.816
36.814
36.812
36.81
-76.3
-76.295
-76.29

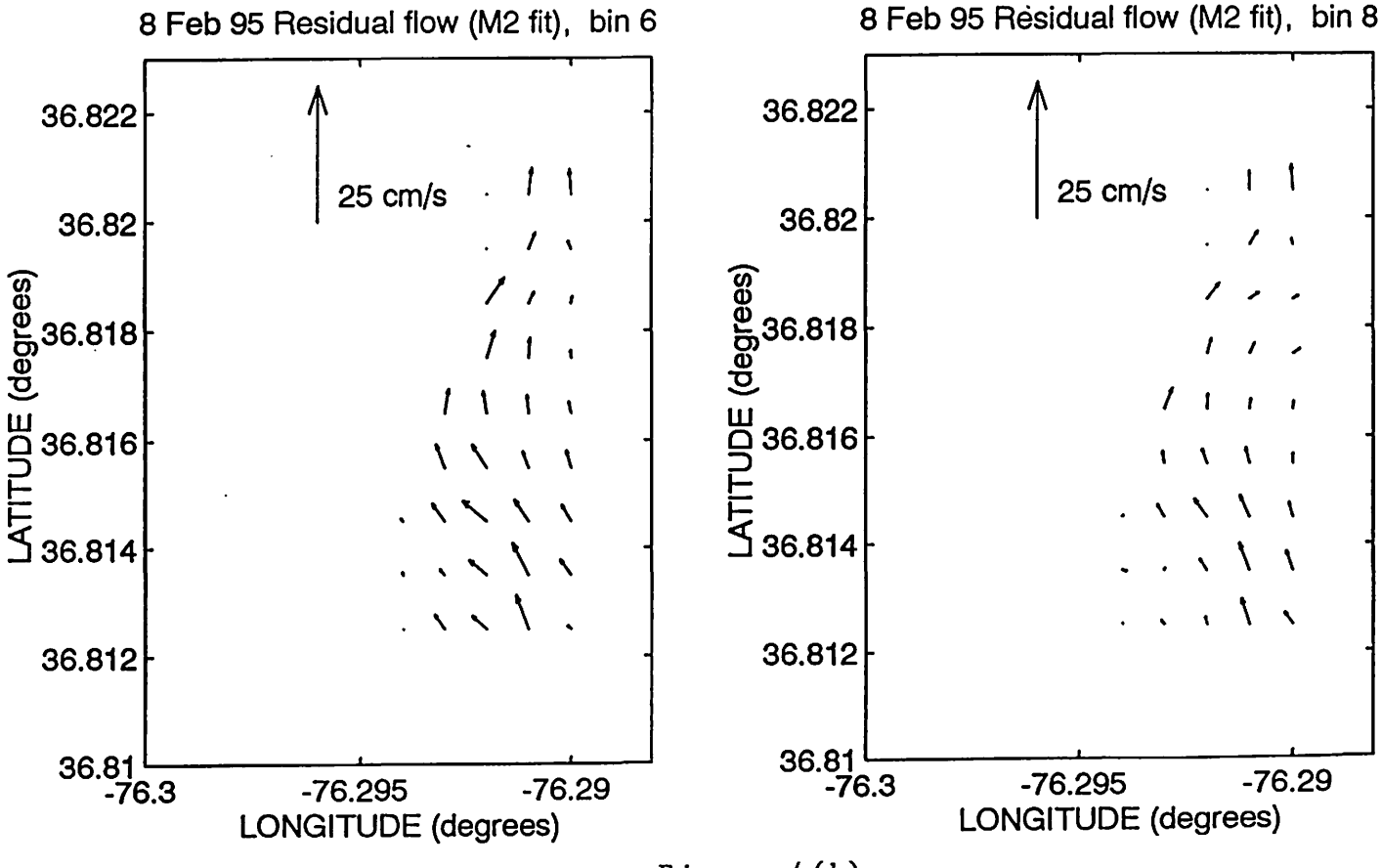
8 Feb 95 Residual flow (M2 fit), bin 6
8 Feb 95 Residual flow (M2 fit), bin 8
25 cm/s
LATITUDE (degrees)
LONGITUDE (degrees)
36.822
36.82
36.818
36.816
36.814
36.812
36.81
-76.3
-76.295
-76.29

Figure 4(b)

APPENDIX

Vector maps representing the flow field as measured on individual surveys. For each survey, data from bins 2 and 8, corresponding to depths of 3 and 9 m, are shown.

1 February 1995, spring tide: 10 surveys.

8 February 1995, neap tide: 11 surveys.

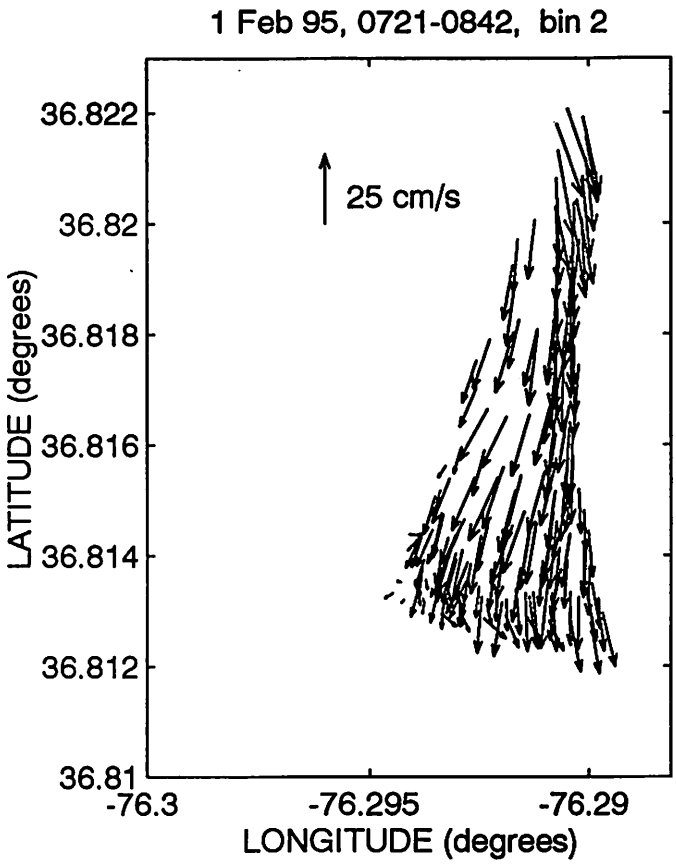
1 Feb 95, 0721-0842, bin 2
25 cm/s
36.822
36.82
36.818
36.816
36.814
36.812
36.81
LATITUDE (degrees)
-76.3
-76.295
-76.29
LONGITUDE (degrees)

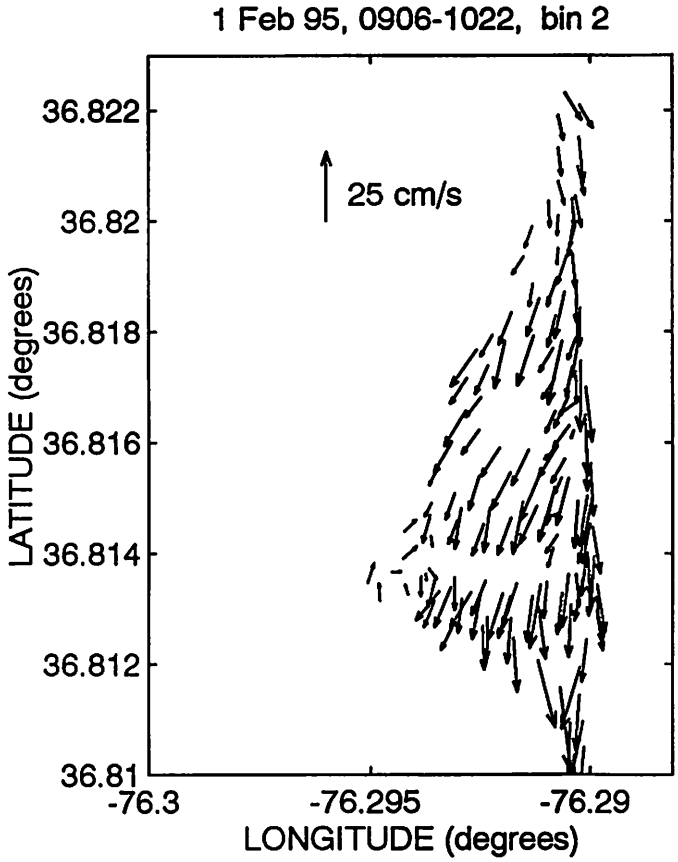
1 Feb 95, 0906-1022, bin 2
25 cm/s
36.822
36.82
36.818
36.816
36.814
36.812
36.81
LATITUDE (degrees)
-76.3
-76.295
-76.29
LONGITUDE (degrees)

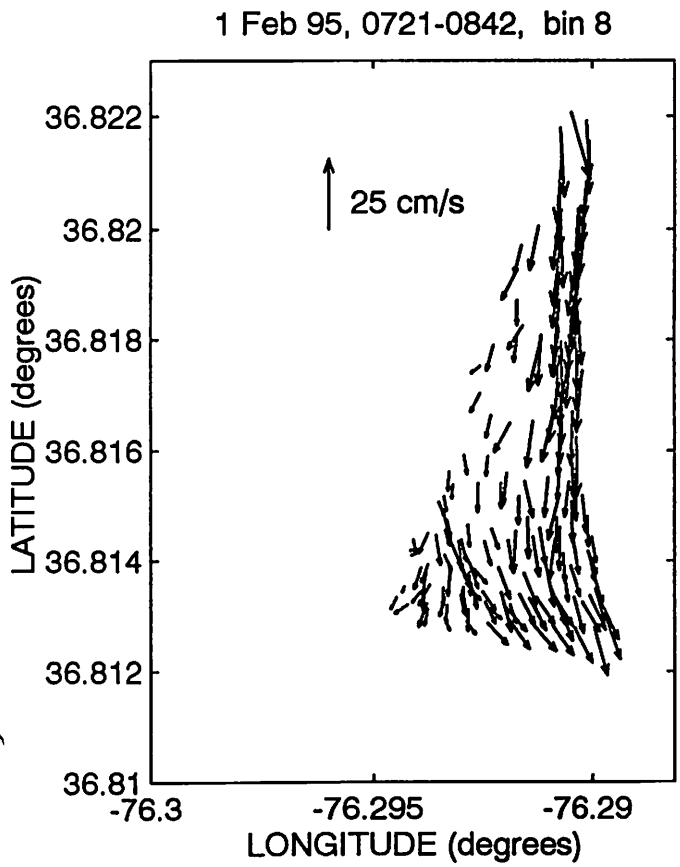
1 Feb 95, 0721-0842, bin 8
25 cm/s
36.822
36.82
36.818
36.816
36.814
36.812
36.81
LATITUDE (degrees)
-76.3
-76.295
-76.29
LONGITUDE (degrees)

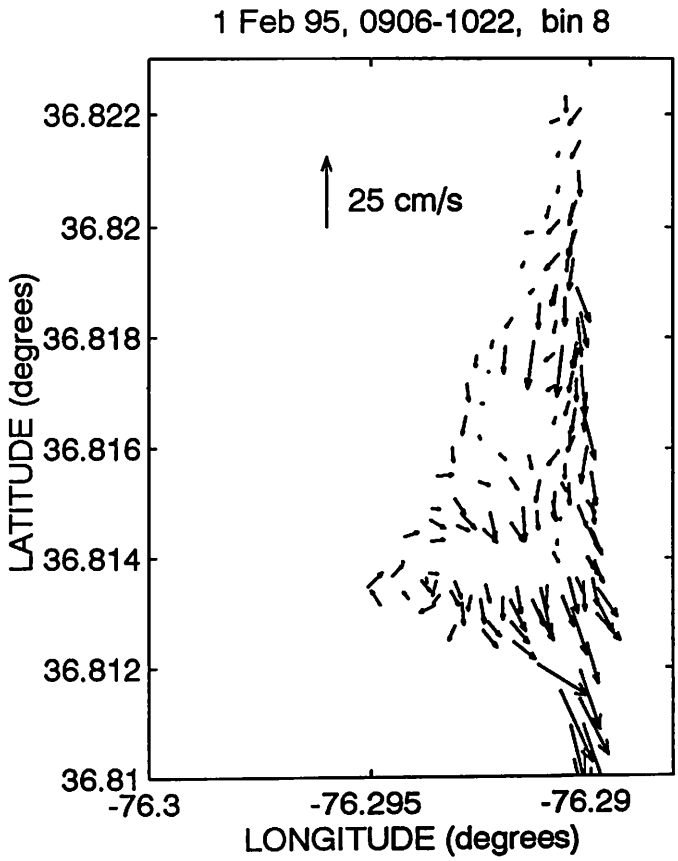
1 Feb 95, 0906-1022, bin 8
25 cm/s
36.822
36.82
36.818
36.816
36.814
36.812
36.81
LATITUDE (degrees)
-76.3
-76.295
-76.29
LONGITUDE (degrees)

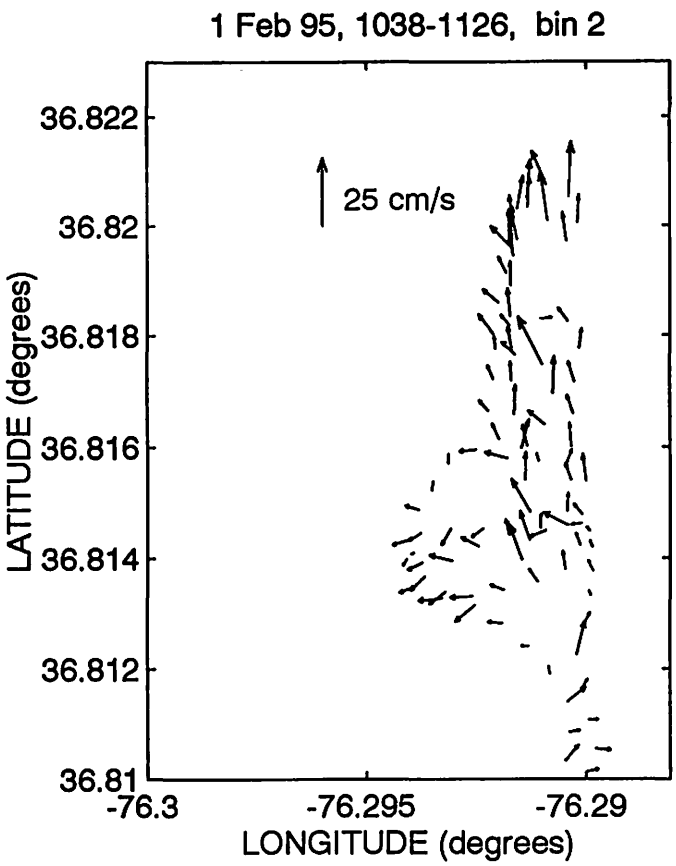
1 Feb 95, 1038-1126, bin 2
25 cm/s
36.822
36.82
36.818
36.816
36.814
36.812
36.81
LATITUDE (degrees)
-76.3
-76.295
-76.29
LONGITUDE (degrees)

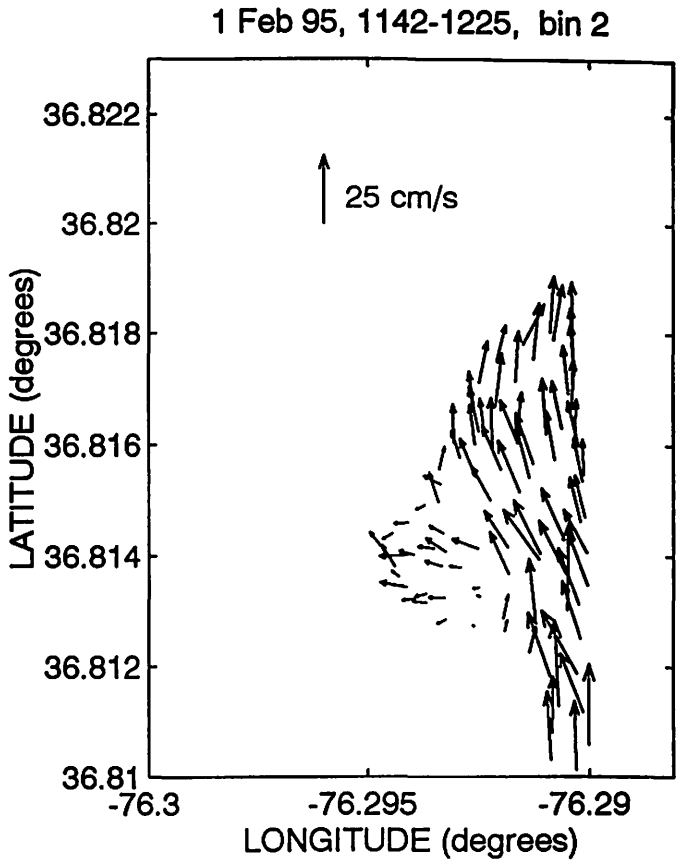
1 Feb 95, 1142-1225, bin 2
25 cm/s
36.822
36.82
36.818
36.816
36.814
36.812
36.81
LATITUDE (degrees)
-76.3
-76.295
-76.29
LONGITUDE (degrees)

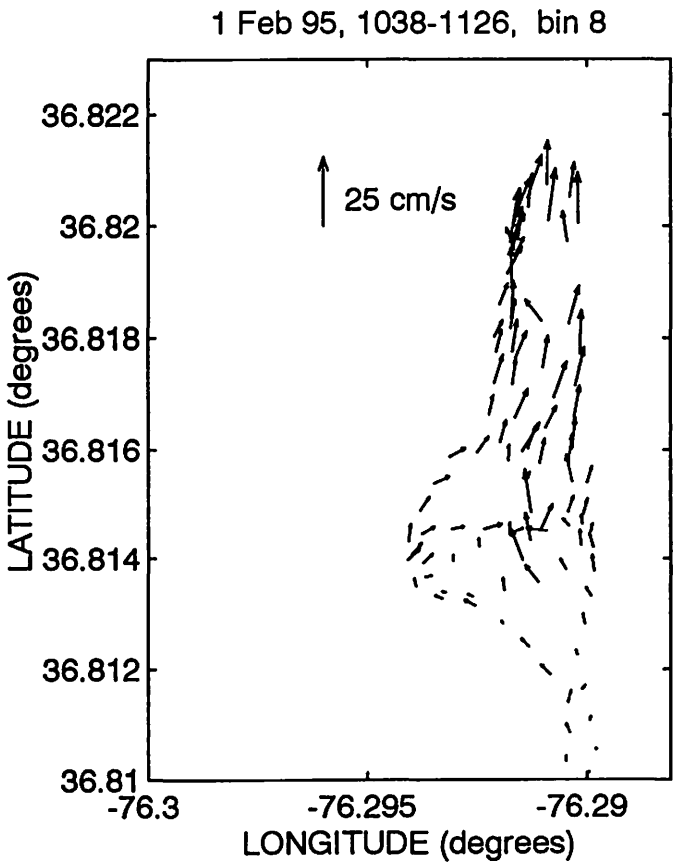
1 Feb 95, 1038-1126, bin 8
25 cm/s
36.822
36.82
36.818
36.816
36.814
36.812
36.81
LATITUDE (degrees)
-76.3
-76.295
-76.29
LONGITUDE (degrees)

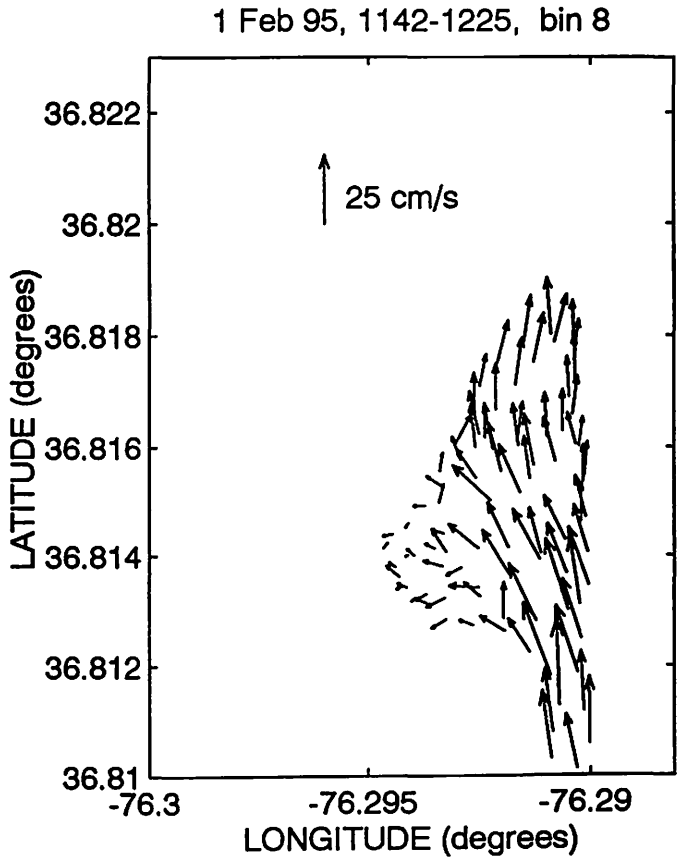
1 Feb 95, 1142-1225, bin 8
25 cm/s
36.822
36.82
36.818
36.816
36.814
36.812
36.81
LATITUDE (degrees)
-76.3
-76.295
-76.29
LONGITUDE (degrees)

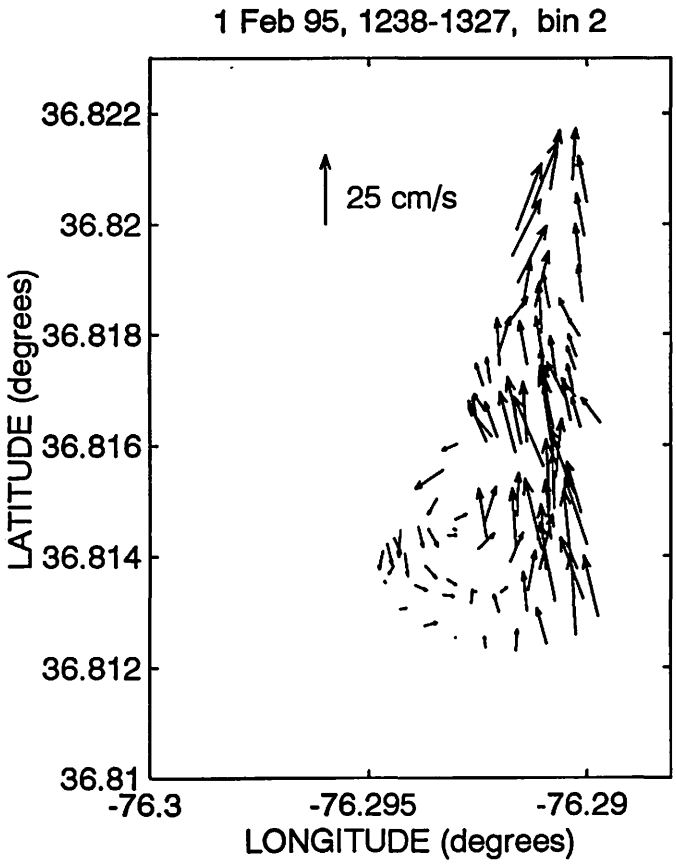
1 Feb 95, 1238-1327, bin 2
25 cm/s
36.822
36.82
36.818
36.816
36.814
36.812
36.81
LATITUDE (degrees)
-76.3
-76.295
-76.29
LONGITUDE (degrees)

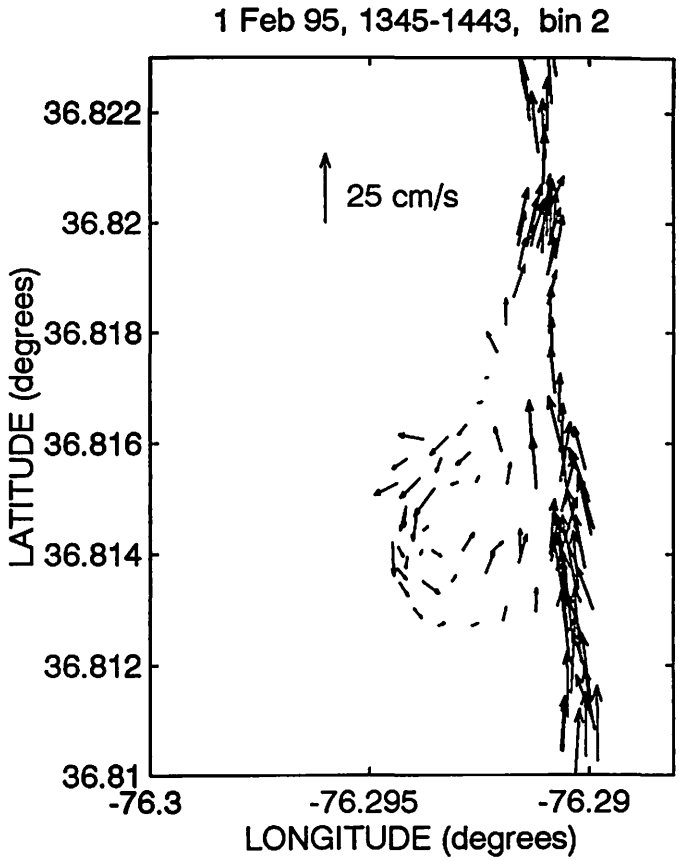
1 Feb 95, 1345-1443, bin 2
25 cm/s
36.822
36.82
36.818
36.816
36.814
36.812
36.81
LATITUDE (degrees)
-76.3
-76.295
-76.29
LONGITUDE (degrees)

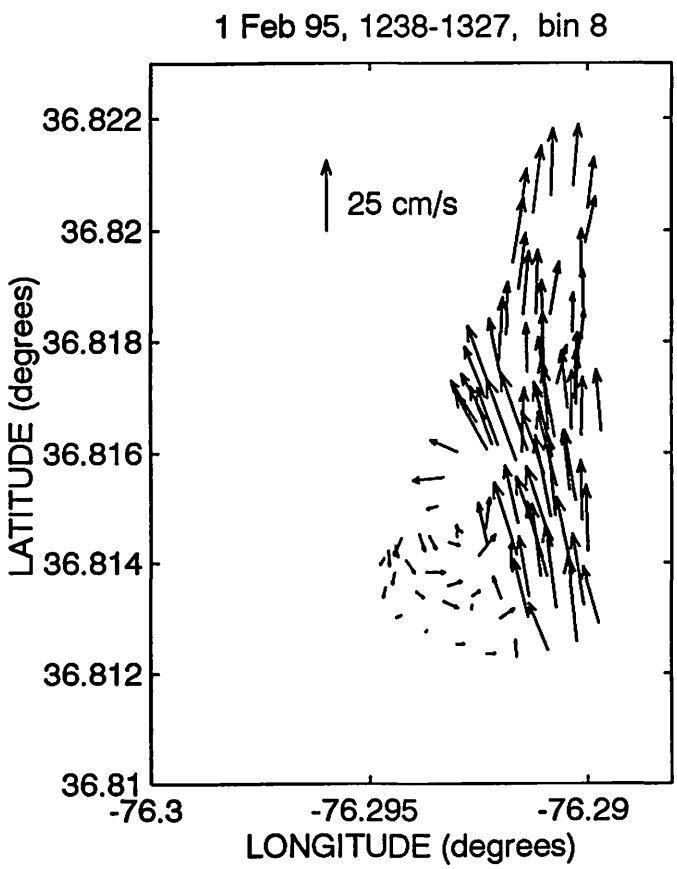
1 Feb 95, 1238-1327, bin 8
25 cm/s
36.822
36.82
36.818
36.816
36.814
36.812
36.81
LATITUDE (degrees)
-76.3
-76.295
-76.29
LONGITUDE (degrees)

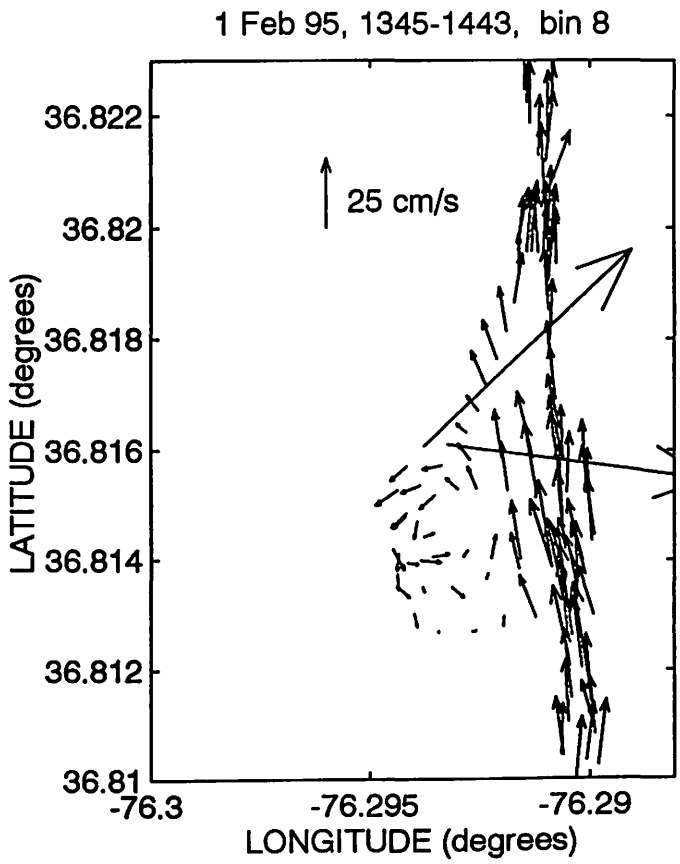
1 Feb 95, 1345-1443, bin 8
25 cm/s
36.822
36.82
36.818
36.816
36.814
36.812
36.81
LATITUDE (degrees)
-76.3
-76.295
-76.29
LONGITUDE (degrees)

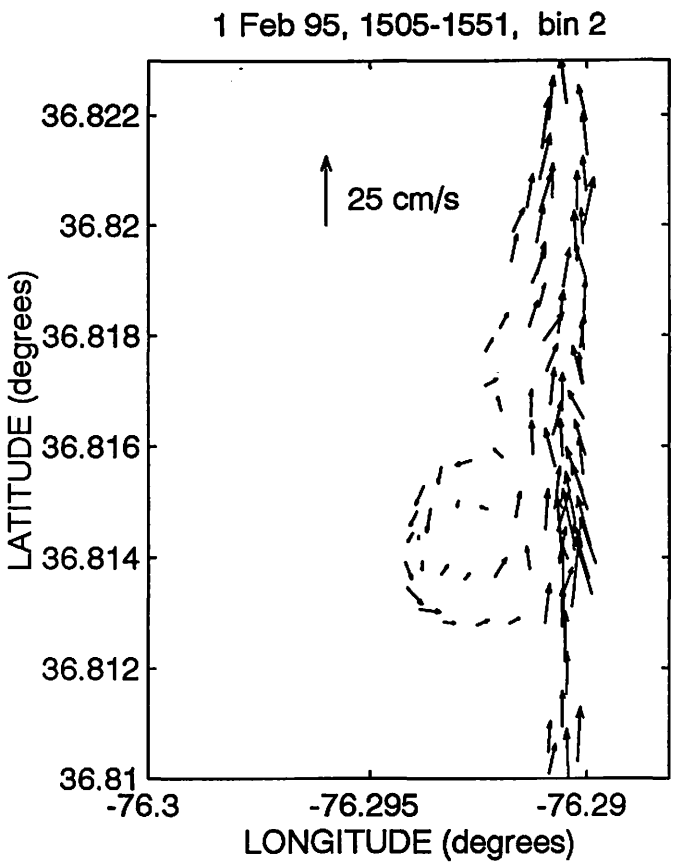
1 Feb 95, 1505-1551, bin 2
25 cm/s
36.822
36.82
36.818
36.816
36.814
36.812
36.81
LATITUDE (degrees)
-76.3
-76.295
-76.29
LONGITUDE (degrees)

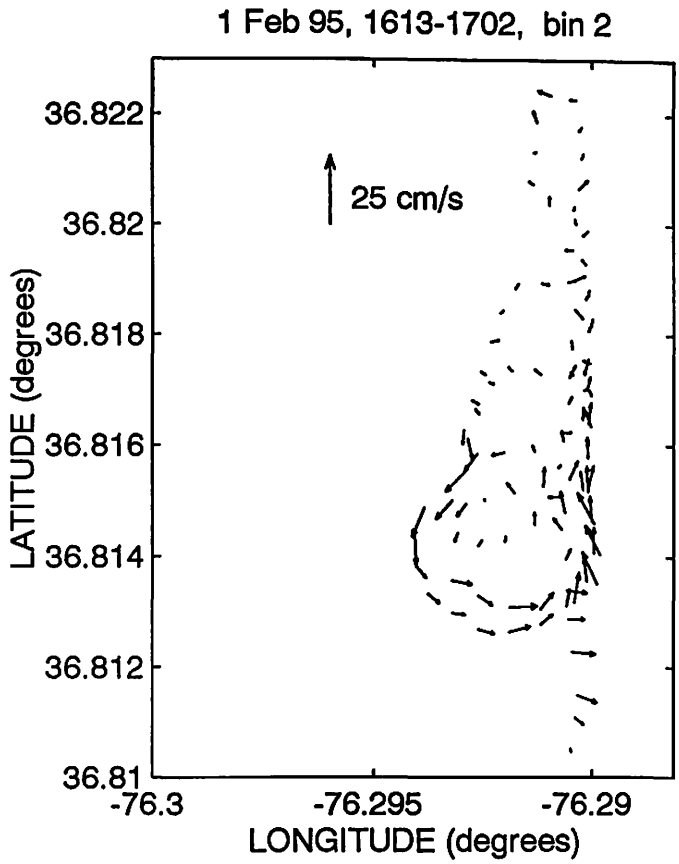
1 Feb 95, 1613-1702, bin 2
25 cm/s
36.822
36.82
36.818
36.816
36.814
36.812
36.81
LATITUDE (degrees)
-76.3
-76.295
-76.29
LONGITUDE (degrees)

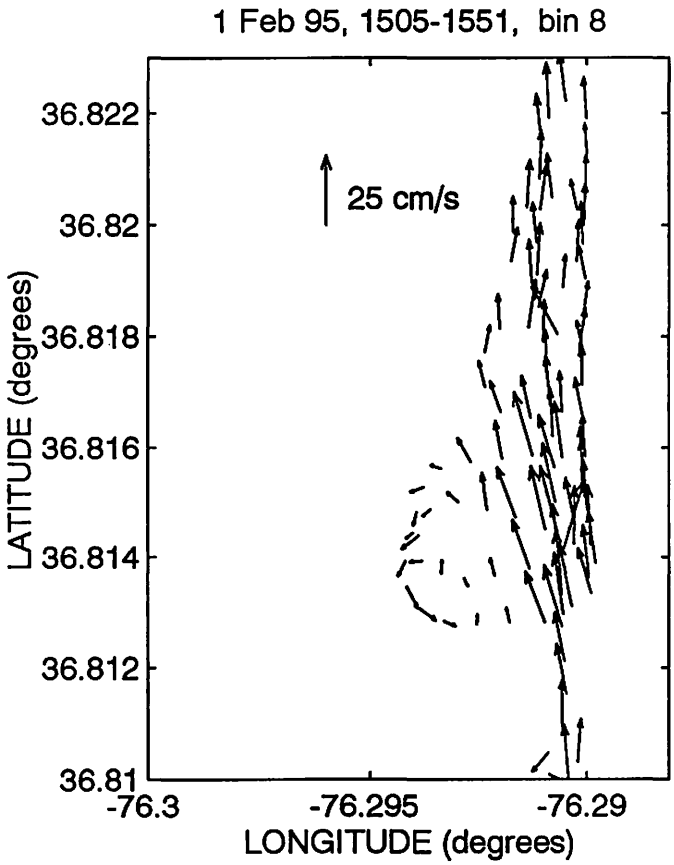
1 Feb 95, 1505-1551, bin 8
25 cm/s
36.822
36.82
36.818
36.816
36.814
36.812
36.81
LATITUDE (degrees)
-76.3
-76.295
-76.29
LONGITUDE (degrees)

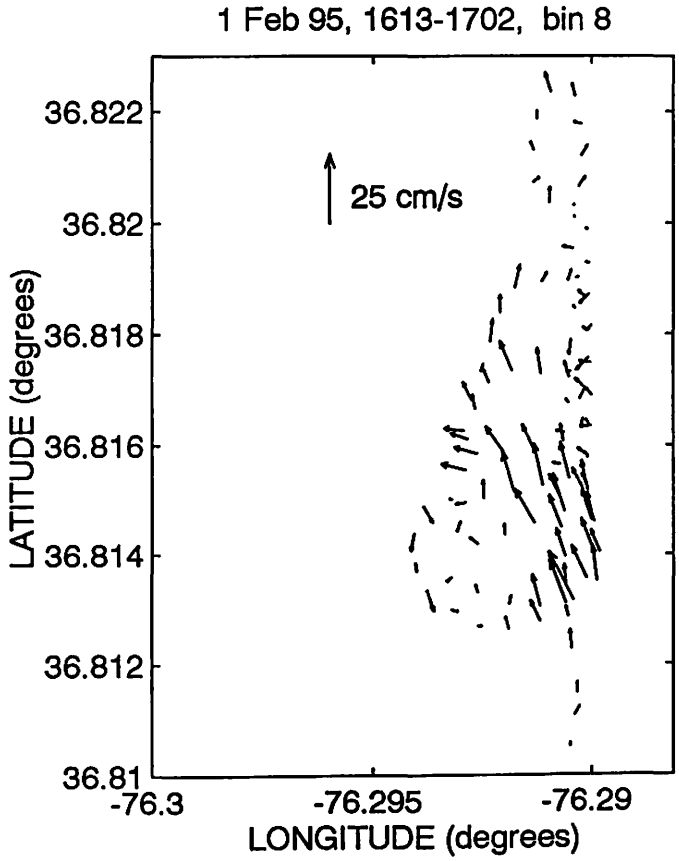
1 Feb 95, 1613-1702, bin 8
25 cm/s
36.822
36.82
36.818
36.816
36.814
36.812
36.81
LATITUDE (degrees)
-76.3
-76.295
-76.29
LONGITUDE (degrees)

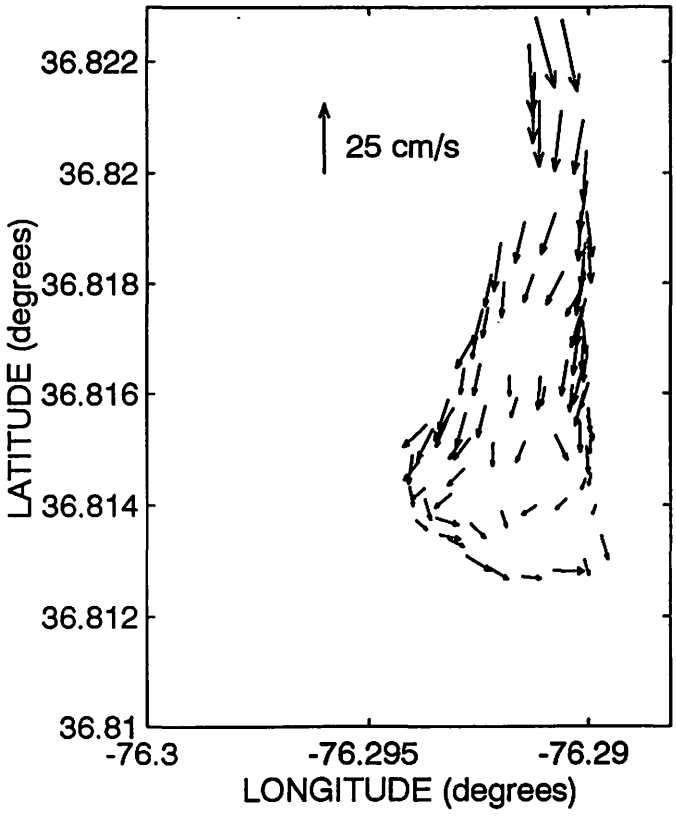
1 Feb 95, 1727-1809, bin 2
25 cm/s
36.822
36.82
36.818
36.816
36.814
36.812
36.81
LATITUDE (degrees)
-76.3
-76.295
-76.29
LONGITUDE (degrees)

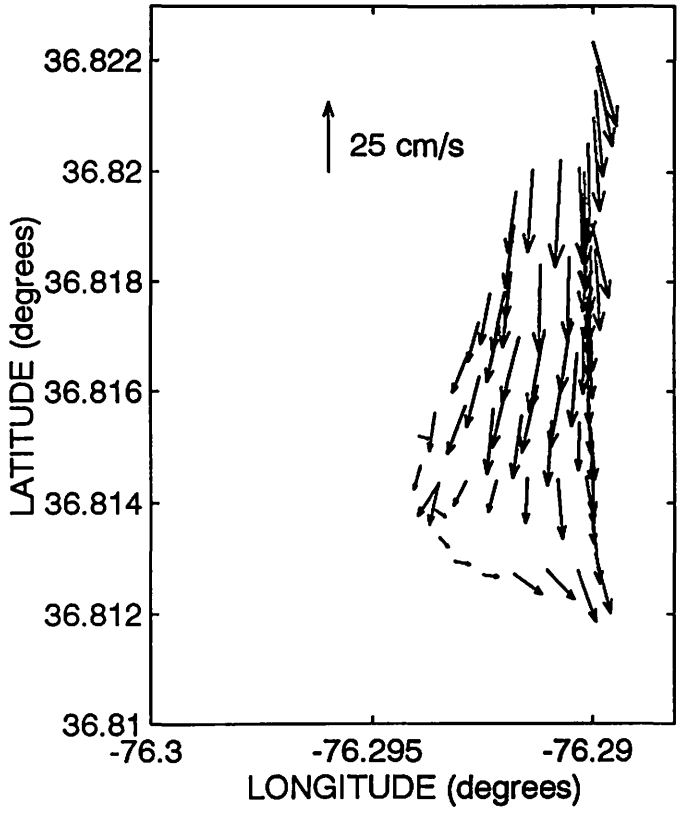
1 Feb 95, 1846-1923, bin 2
25 cm/s
36.822
36.82
36.818
36.816
36.814
36.812
36.81
LATITUDE (degrees)
-76.3
-76.295
-76.29
LONGITUDE (degrees)

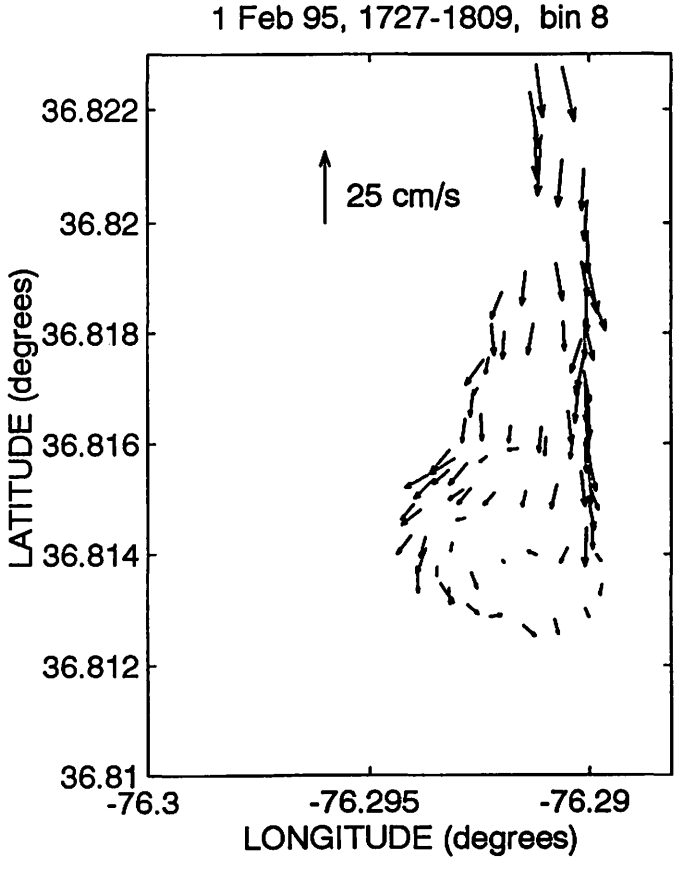
1 Feb 95, 1727-1809, bin 8
25 cm/s
36.822
36.82
36.818
36.816
36.814
36.812
36.81
LATITUDE (degrees)
-76.3
-76.295
-76.29
LONGITUDE (degrees)

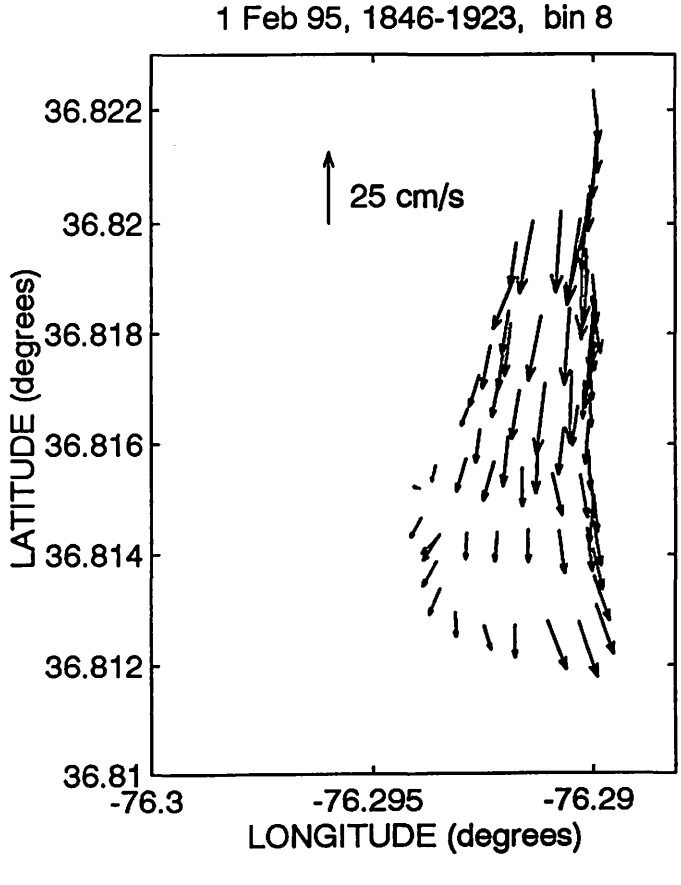
1 Feb 95, 1846-1923, bin 8
25 cm/s
36.822
36.82
36.818
36.816
36.814
36.812
36.81
LATITUDE (degrees)
-76.3
-76.295
-76.29
LONGITUDE (degrees)

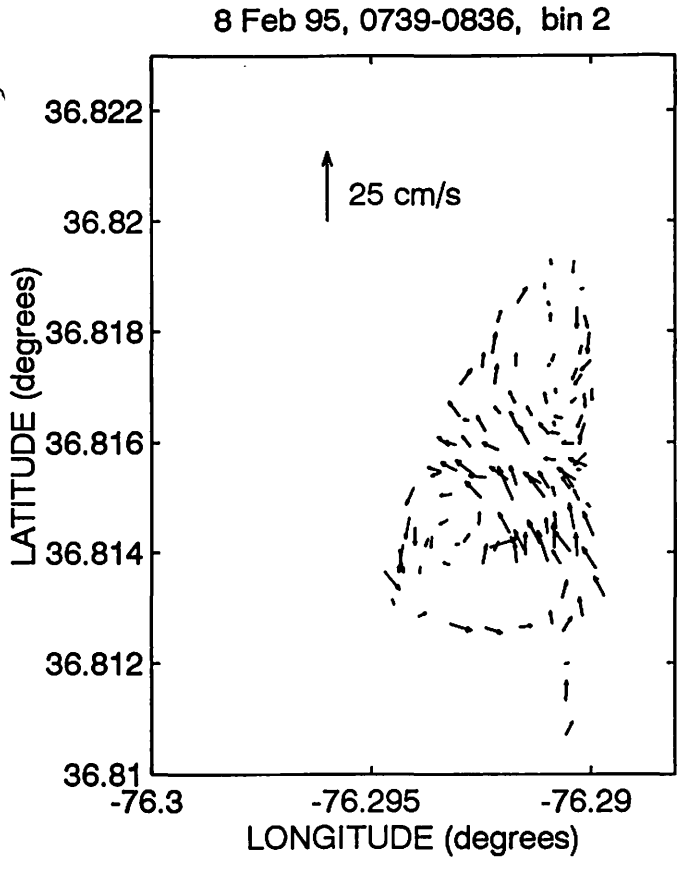
8 Feb 95, 0739-0836, bin 2
25 cm/s
36.822
36.82
36.818
36.816
36.814
36.812
36.81
LATITUDE (degrees)
-76.3
-76.295
-76.29
LONGITUDE (degrees)

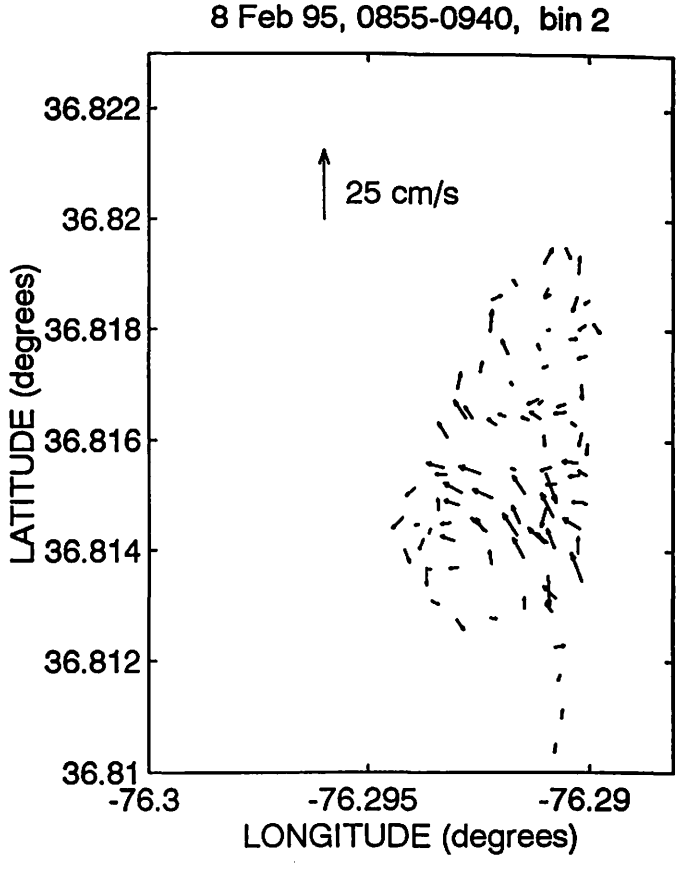
8 Feb 95, 0855-0940, bin 2
25 cm/s
36.822
36.82
36.818
36.816
36.814
36.812
36.81
LATITUDE (degrees)
-76.3
-76.295
-76.29
LONGITUDE (degrees)

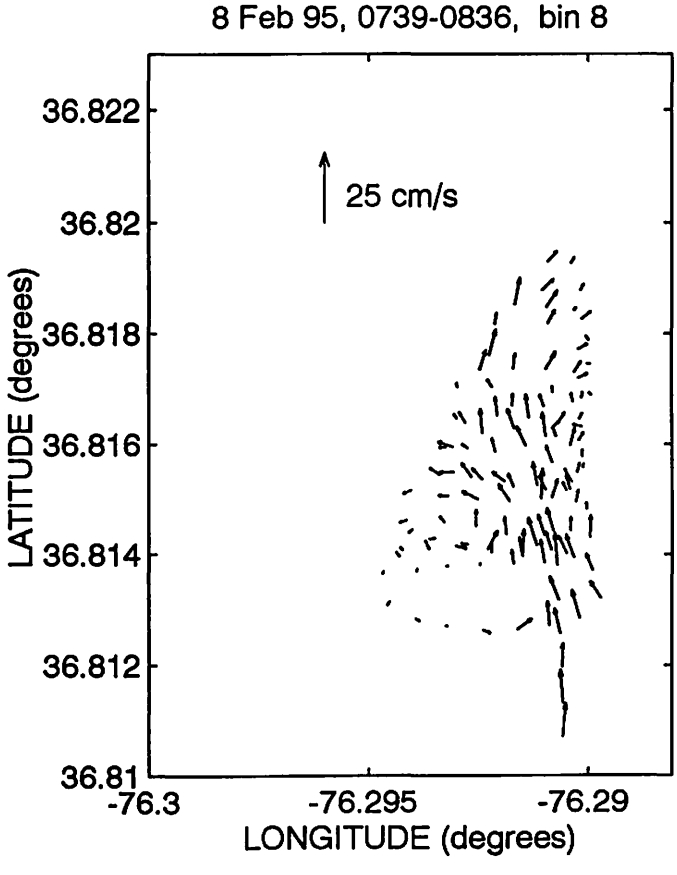
8 Feb 95, 0739-0836, bin 8
25 cm/s
36.822
36.82
36.818
36.816
36.814
36.812
36.81
LATITUDE (degrees)
-76.3
-76.295
-76.29
LONGITUDE (degrees)

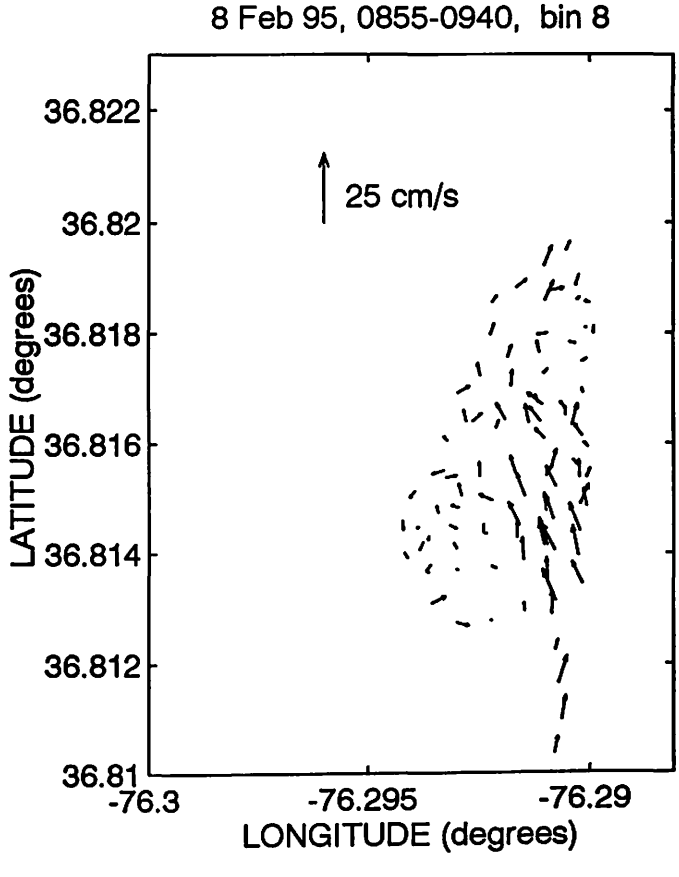
8 Feb 95, 0855-0940, bin 8
25 cm/s
36.822
36.82
36.818
36.816
36.814
36.812
36.81
LATITUDE (degrees)
-76.3
-76.295
-76.29
LONGITUDE (degrees)

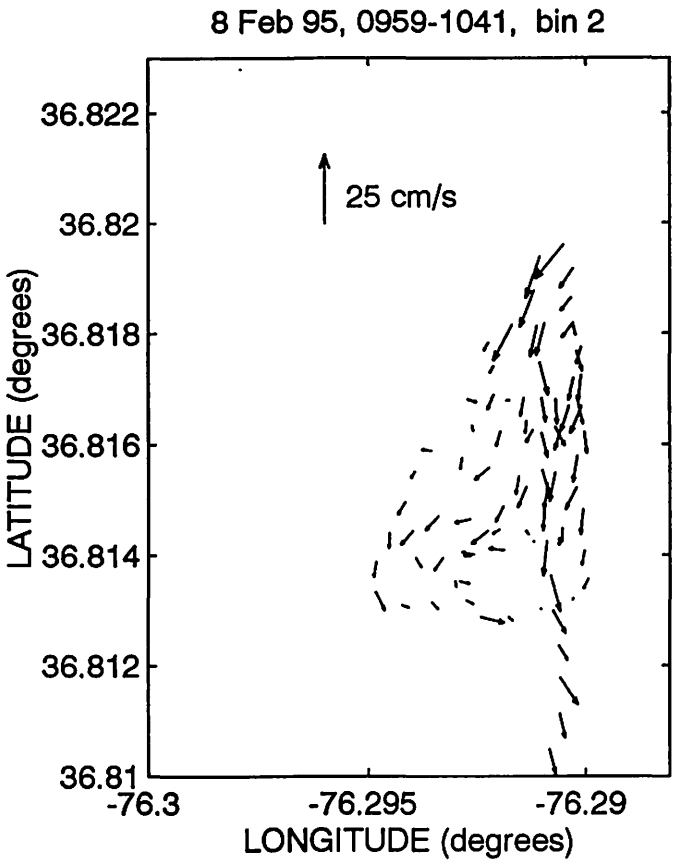
8 Feb 95, 0959-1041, bin 2
25 cm/s
36.822
36.82
36.818
36.816
36.814
36.812
36.81
LATITUDE (degrees)
-76.3
-76.295
-76.29
LONGITUDE (degrees)

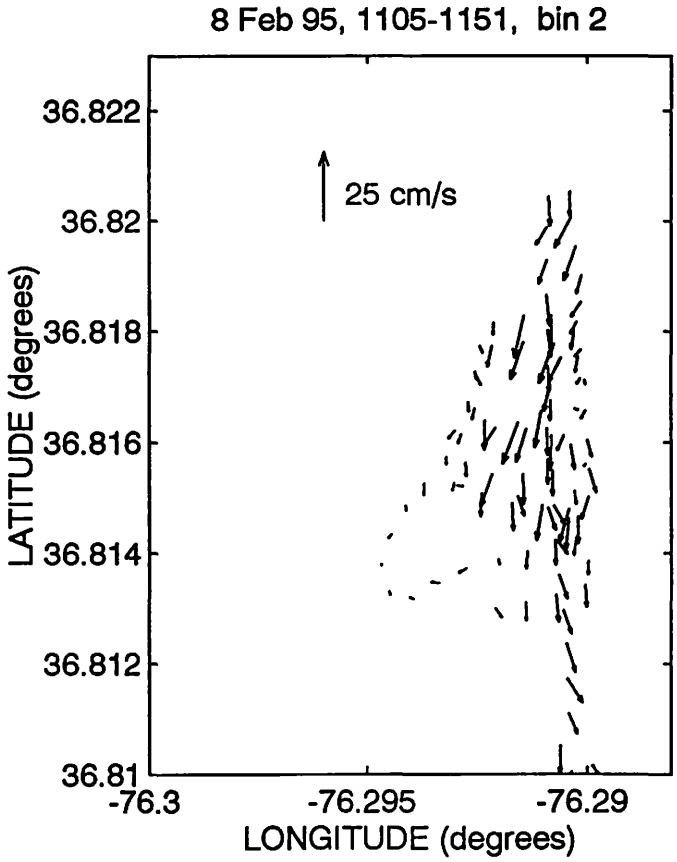
8 Feb 95, 1105-1151, bin 2
25 cm/s
36.822
36.82
36.818
36.816
36.814
36.812
36.81
LATITUDE (degrees)
-76.3
-76.295
-76.29
LONGITUDE (degrees)

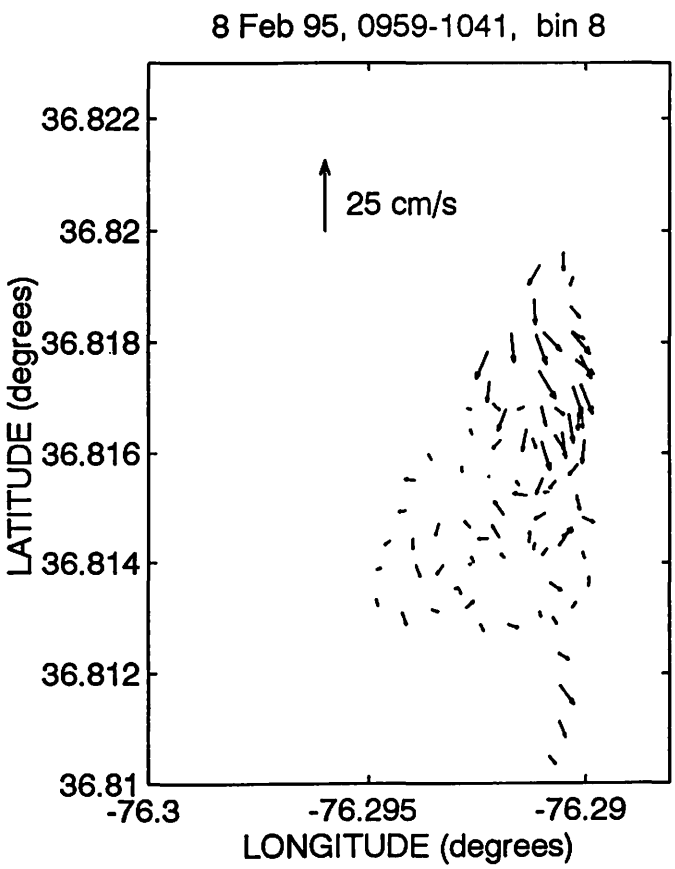
8 Feb 95, 0959-1041, bin 8
25 cm/s
36.822
36.82
36.818
36.816
36.814
36.812
36.81
LATITUDE (degrees)
-76.3
-76.295
-76.29
LONGITUDE (degrees)

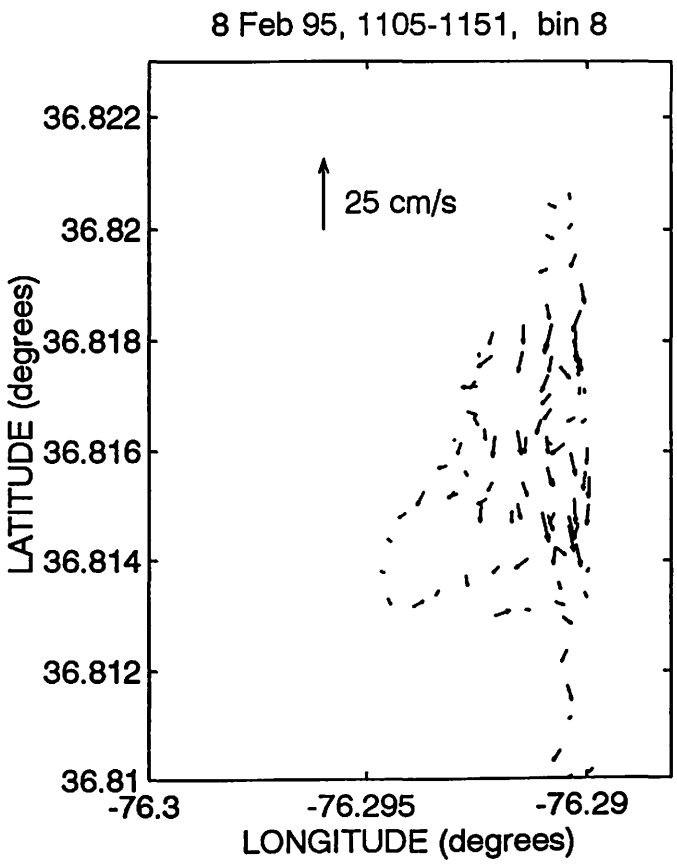
8 Feb 95, 1105-1151, bin 8
25 cm/s
36.822
36.82
36.818
36.816
36.814
36.812
36.81
LATITUDE (degrees)
-76.3
-76.295
-76.29
LONGITUDE (degrees)

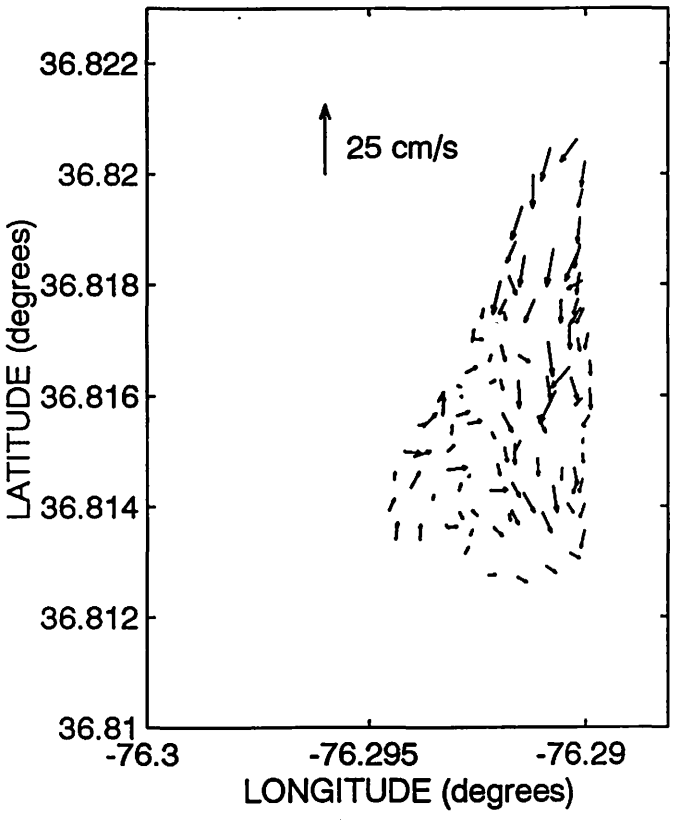
8 Feb 95, 1210-1301, bin 2
25 cm/s
36.822
36.82
36.818
36.816
36.814
36.812
36.81
LATITUDE (degrees)
-76.3
-76.295
-76.29
LONGITUDE (degrees)

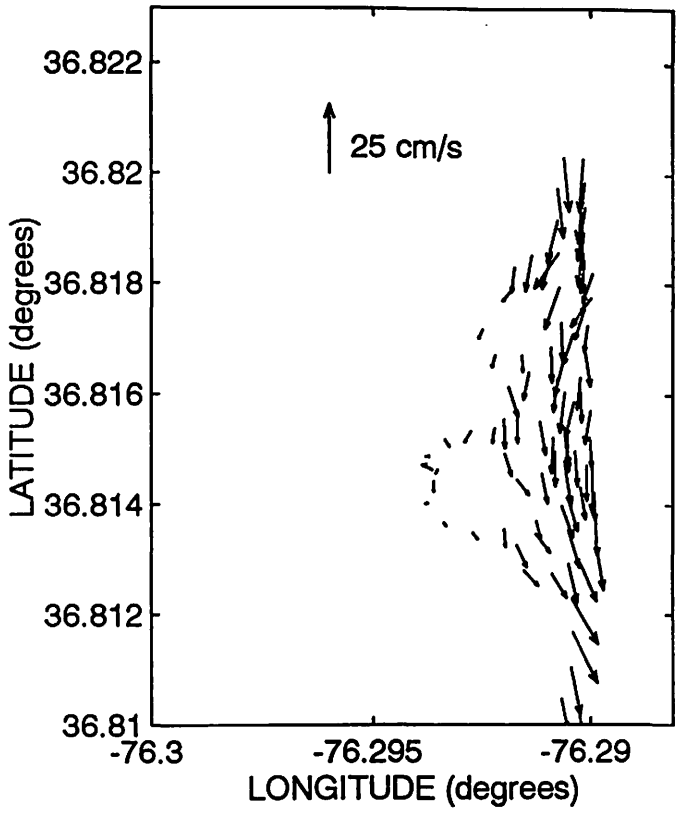
8 Feb 95, 1315-1355, bin 2
25 cm/s
36.822
36.82
36.818
36.816
36.814
36.812
36.81
LATITUDE (degrees)
-76.3
-76.295
-76.29
LONGITUDE (degrees)

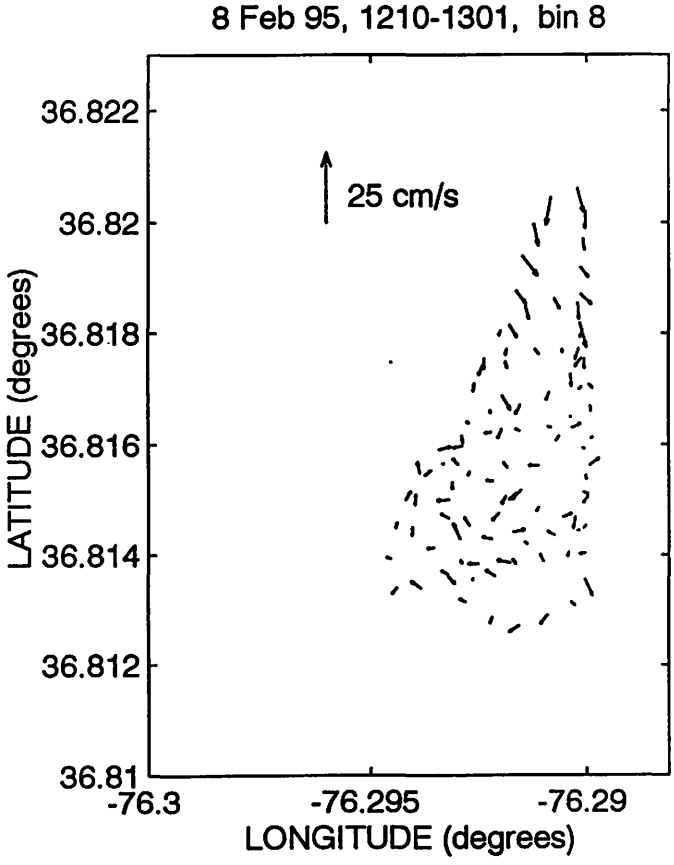
8 Feb 95, 1210-1301, bin 8
25 cm/s
36.822
36.82
36.818
36.816
36.814
36.812
36.81
LATITUDE (degrees)
-76.3
-76.295
-76.29
LONGITUDE (degrees)

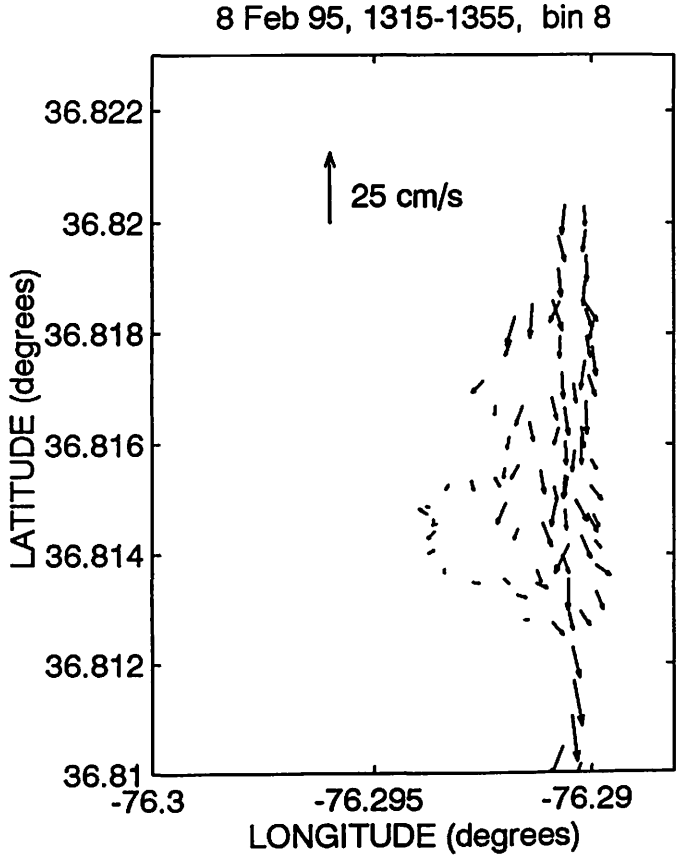
8 Feb 95, 1315-1355, bin 8
25 cm/s
36.822
36.82
36.818
36.816
36.814
36.812
36.81
LATITUDE (degrees)
-76.3
-76.295
-76.29
LONGITUDE (degrees)

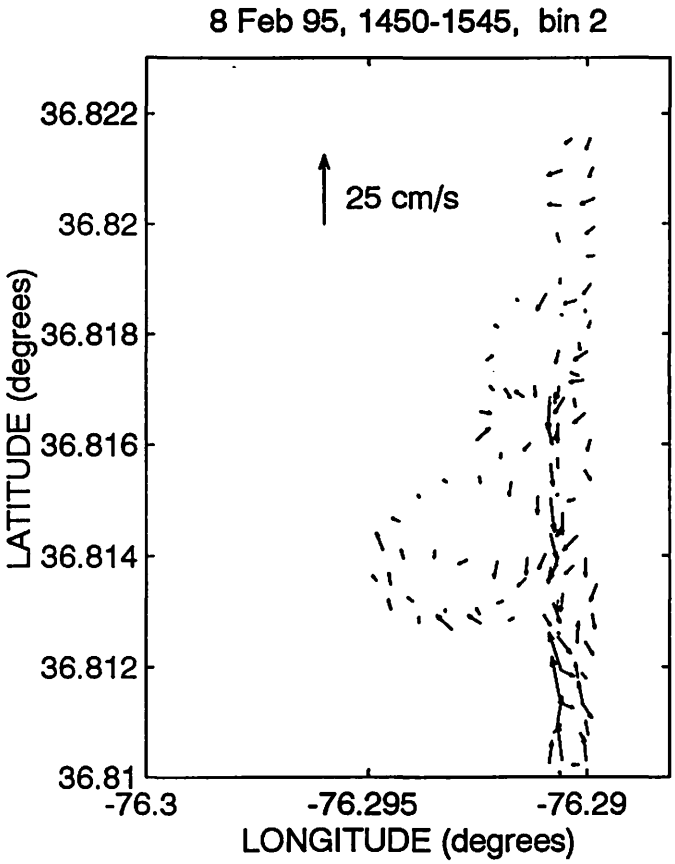
8 Feb 95, 1450-1545, bin 2
25 cm/s
36.822
36.82
36.818
36.816
36.814
36.812
36.81
LATITUDE (degrees)
-76.3
-76.295
-76.29
LONGITUDE (degrees)

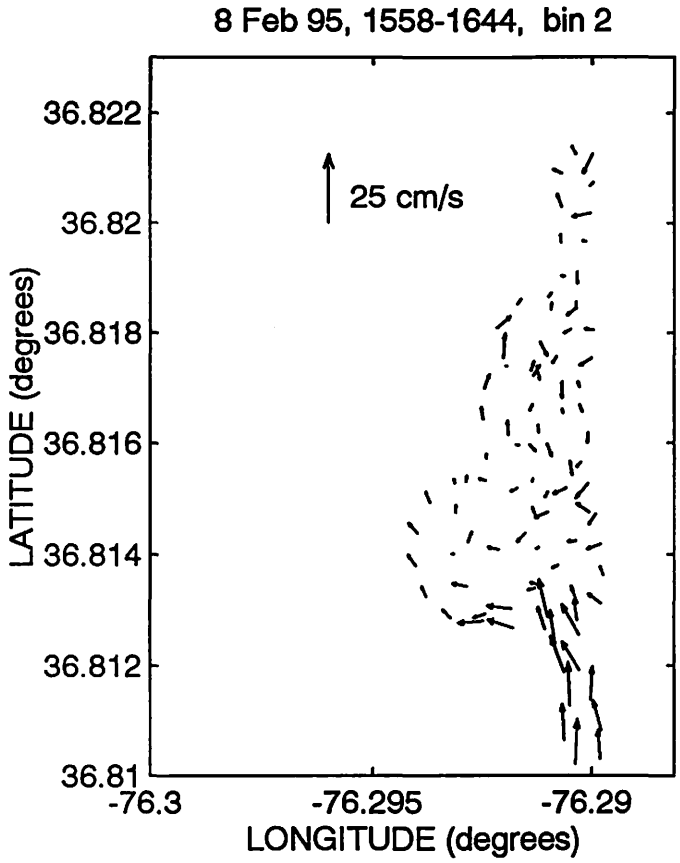
8 Feb 95, 1558-1644, bin 2
25 cm/s
36.822
36.82
36.818
36.816
36.814
36.812
36.81
LATITUDE (degrees)
-76.3
-76.295
-76.29
LONGITUDE (degrees)

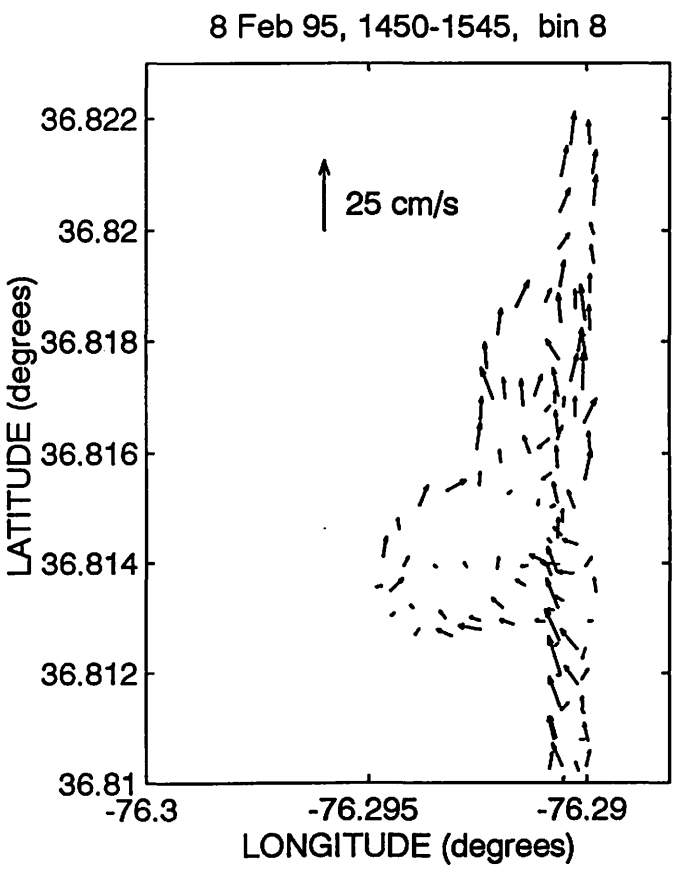
8 Feb 95, 1450-1545, bin 8
25 cm/s
36.822
36.82
36.818
36.816
36.814
36.812
36.81
LATITUDE (degrees)
-76.3
-76.295
-76.29
LONGITUDE (degrees)

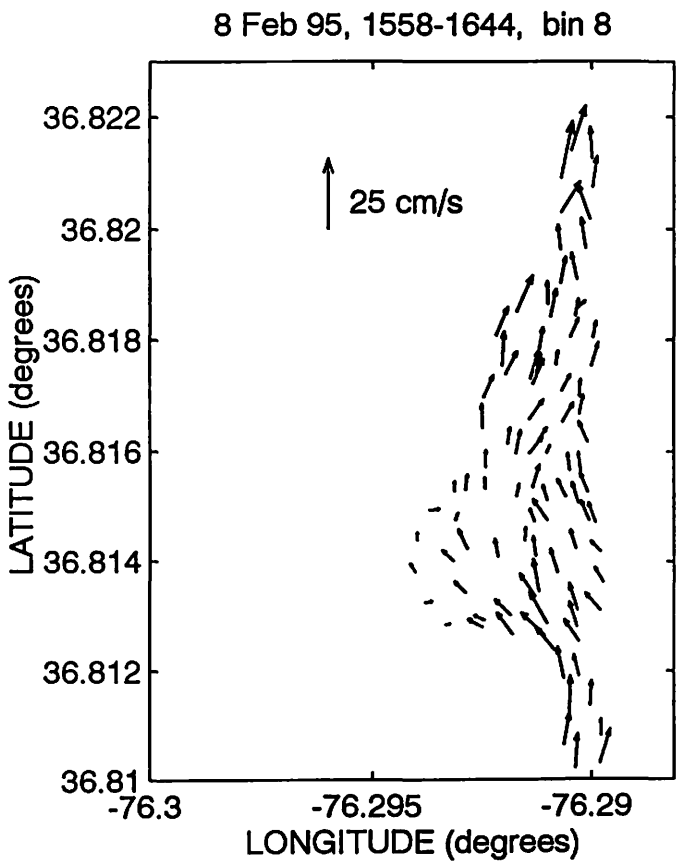
8 Feb 95, 1558-1644, bin 8
25 cm/s
36.822
36.82
36.818
36.816
36.814
36.812
36.81
LATITUDE (degrees)
-76.3
-76.295
-76.29
LONGITUDE (degrees)

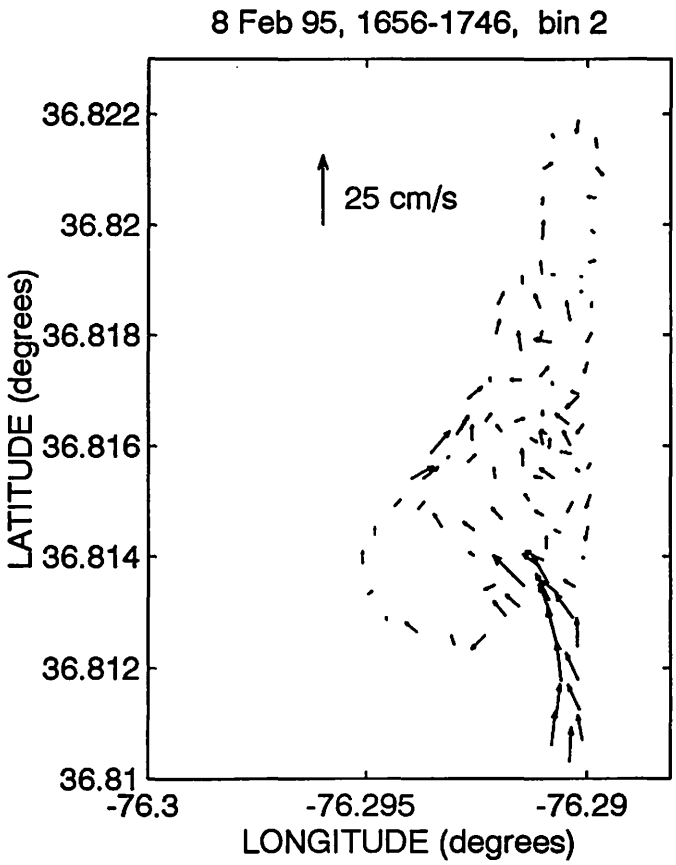
8 Feb 95, 1656-1746, bin 2
25 cm/s
36.822
36.82
36.818
36.816
36.814
36.812
36.81
LATITUDE (degrees)
-76.3
-76.295
-76.29
LONGITUDE (degrees)

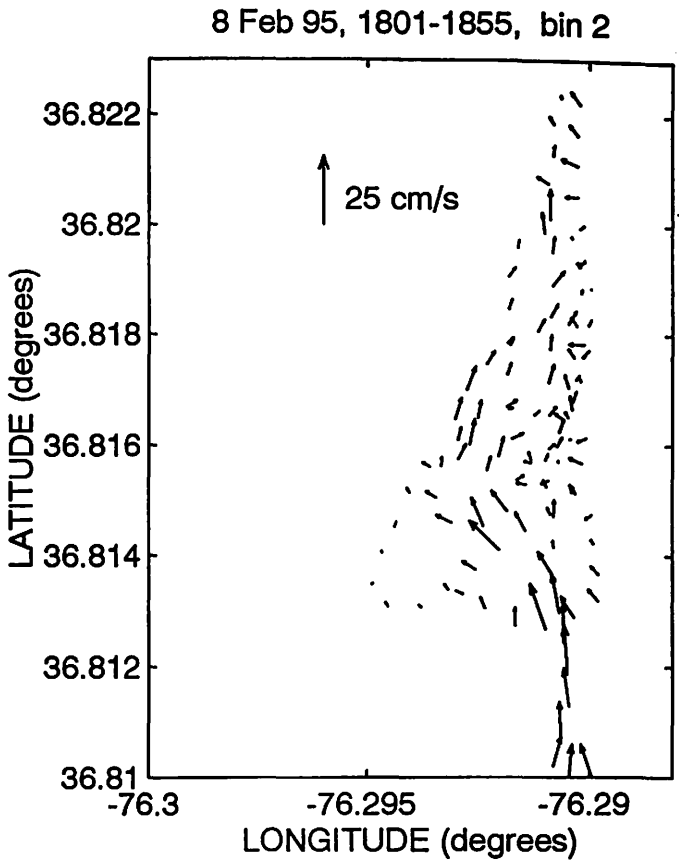
8 Feb 95, 1801-1855, bin 2
25 cm/s
36.822
36.82
36.818
36.816
36.814
36.812
36.81
LATITUDE (degrees)
-76.3
-76.295
-76.29
LONGITUDE (degrees)

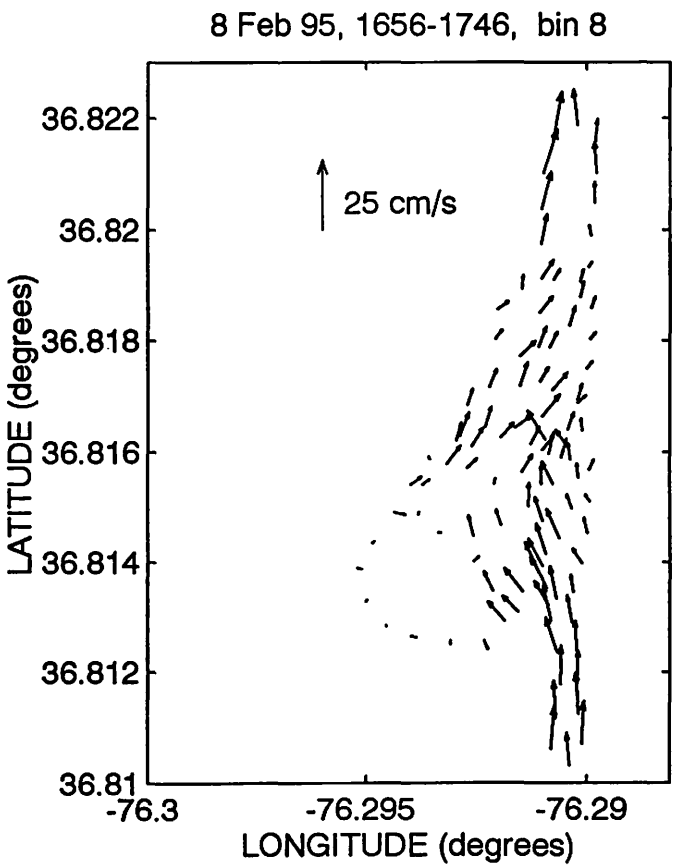
8 Feb 95, 1656-1746, bin 8
25 cm/s
36.822
36.82
36.818
36.816
36.814
36.812
36.81
LATITUDE (degrees)
-76.3
-76.295
-76.29
LONGITUDE (degrees)

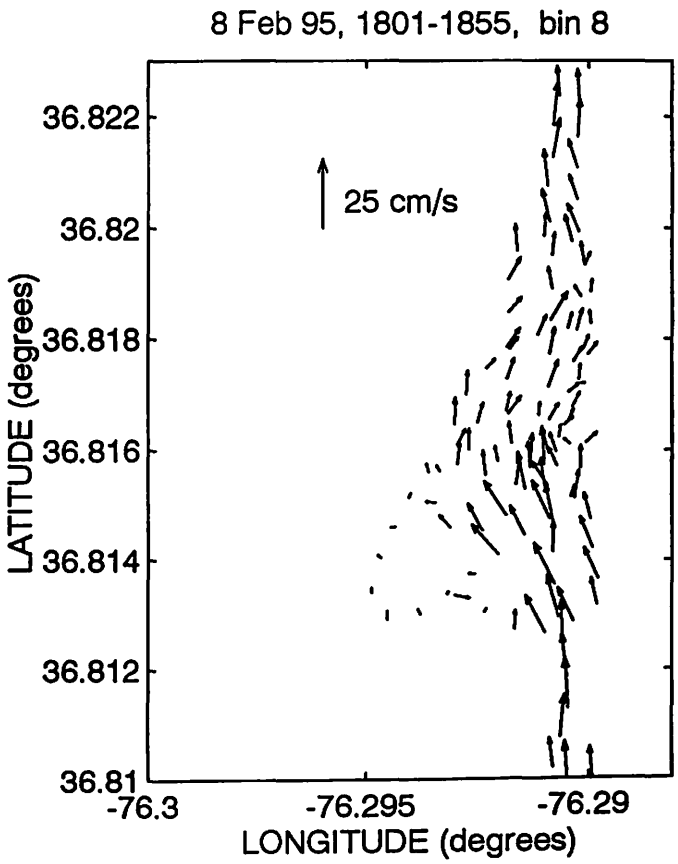
8 Feb 95, 1801-1855, bin 8
25 cm/s
36.822
36.82
36.818
36.816
36.814
36.812
36.81
LATITUDE (degrees)
-76.3
-76.295
-76.29
LONGITUDE (degrees)

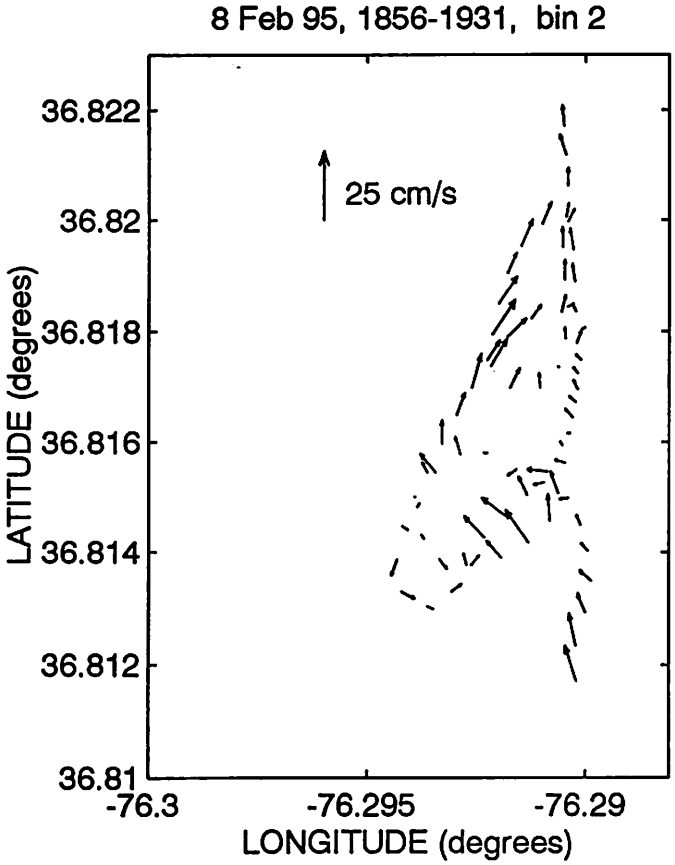
8 Feb 95, 1856-1931, bin 2
25 cm/s
36.822
36.82
36.818
36.816
36.814
36.812
36.81
LATITUDE (degrees)
-76.3
-76.295
-76.29
LONGITUDE (degrees)

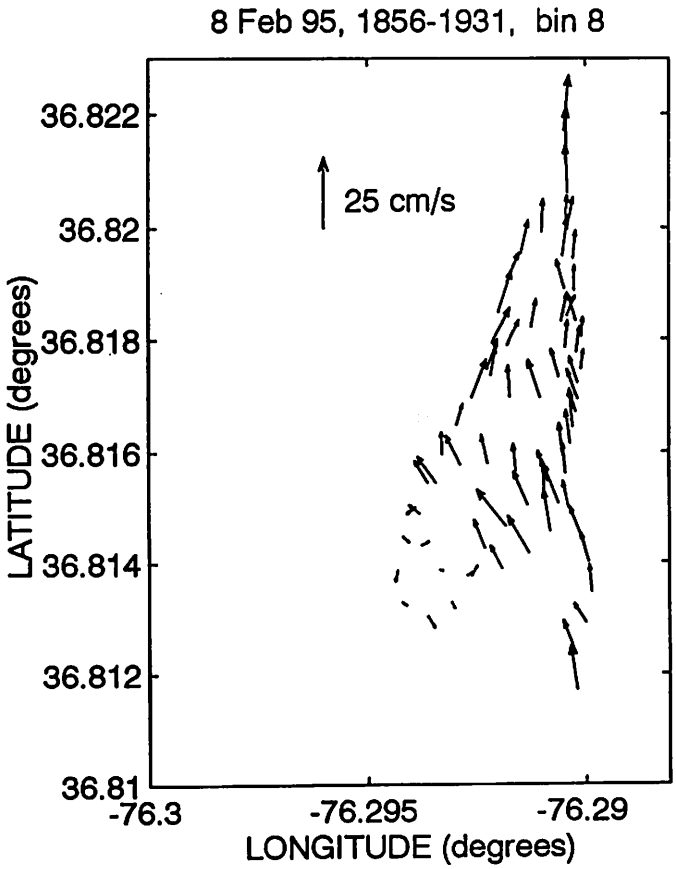
8 Feb 95, 1856-1931, bin 8
25 cm/s
36.822
36.82
36.818
36.816
36.814
36.812
36.81
LATITUDE (degrees)
-76.3
-76.295
-76.29
LONGITUDE (degrees)